NASA TECHNICAL NOTE

NASA TN D-5432

C. 1

NASA TN D-5432

RESIDUAL TENSILE STRENGTH IN THE PRESENCE OF THROUGH CRACKS OR SURFACE CRACKS

by Paul Kuhn

Langley Research Center
Langley Station, Hampton, Va.

NATIONAL AERONAUTICS AND SPACE ADMINISTRATION • WASHINGTON, D. C. • MARCH 1970

1. Report No. NASA TN D-5432	2. Government Accession No.	3. Recipient's Catalog No.
4. Title and Subtitle RESIDUAL TENSILE STRENGTH IN THE PRESENCE OF THROUGH CRACKS OR SURFACE CRACKS		5. Report Date March 1970 6. Performing Organization Code
7. Author(s) Paul Kuhn		8. Performing Organization Report No. L-6658
9. Performing Organization Name and Address NASA Langley Research Center Langley Station Hampton, Va. 23365		10. Work Unit No. 126-14-15-01-23 11. Contract or Grant No. 13. Type of Report and Period Covered Technical Note
12. Sponsoring Agency Name and Address National Aeronautics and Space Administration Washington, D.C. 20546		14. Sponsoring Agency Code

15. Supplementary Notes

16. Abstract

A method of crack-strength analysis for through cracks previously published is briefly restated and discussed. A formula is then given which, in effect, converts a surface crack into an equivalent through crack so that strength calculations can be made. Twenty-five sets of tests on surface cracks are shown together with predicted curves based on through-crack tests. The predicted strengths are either reasonably close or somewhat conservative.

17. Key Words Suggested by Author(s)	18. Distribution Statement
Structural mechanics Materials, metallic Cracks Fracture strength Fatigue Surface cracks	Unclassified – Unlimited

19. Security Classif. (of this report)	20. Security Classif. (of this page)	21. No. of Pages	22. Price*
Unclassified	Unclassified	40	$3.00

*For sale by the Clearinghouse for Federal Scientific and Technical Information
Springfield, Virginia 22151

RESIDUAL TENSILE STRENGTH IN THE PRESENCE OF THROUGH CRACKS OR SURFACE CRACKS

By Paul Kuhn
Langley Research Center

SUMMARY

A method of crack-strength analysis for through cracks previously published is briefly restated and discussed. A formula is then given which, in effect, converts a surface crack into an equivalent through crack so that strength calculations can be made. Twenty-five sets of tests on surface cracks are shown together with predicted curves based on through-crack tests. The predicted strengths are either reasonably close or somewhat conservative.

INTRODUCTION

In their never-ending quest for higher structural efficiency, designers resort again and again to the use of materials with higher strength-weight ratios. However, experience has shown that higher strength-weight ratios are often accompanied by increased sensitivity to cracks, and if the strength of a given material is near the maximum obtainable by heat treatment or cold work, the crack sensitivity is often intolerably high, that is, catastrophic failures would result from very small cracks. Thus, the designer must strike a very carefully considered compromise between strength and crack sensitivity; in order to do so, he must have an adequate understanding of crack sensitivity. In some branches of structural engineering, a qualitative understanding may be adequate; in others, such as aerospace engineering, a quantitative understanding is becoming highly desirable.

Since there exists at present no fundamental theory of fracture, the approach is of necessity empirical. A vast amount of work has been done on tensile specimens with "through cracks," which penetrate through the entire thickness of the material. More recently, the focus of attention has shifted to surface or "part-through" cracks. This paper presents first a method for correlating through cracks in tensile specimens which has been published previously (refs. 1 and 2), but is included again, partly to make the paper self-contained, and partly to discuss the results of an approximation which is generally necessary at present because of the lack of data. Next, a formula is given which permits the calculation of strength in the presence of a surface crack by defining an "equivalent through-crack length," that is, the length of a through crack which would

result in the same failing load as the surface crack. Experimental data for a number of materials are presented in which a materials constant derived from one or more tests with through cracks is used to predict the strength of a series of surface cracks by means of the equivalent-length formula.

SYMBOLS

The units used for the physical quantities defined in this paper are given both in the U.S. Customary units and in the International System of Units (SI) in appendix A. Factors relating the two systems are given in reference 3.

A_c	area of surface crack
a	half-length of central crack or length of edge crack for through cracks, half-length as measured on the surface for surface cracks
C_m, C_m'	materials constants (expressions (2) and (5))
c	depth of surface crack
K_u, K_u'	stress concentration factors valid at ultimate load as used in expression (1) or (4)
k_w	finite-width factor (expressions (3a) and (3b))
S_G	stress on gross section at ultimate load
S_N	stress on net section at ultimate load
t	thickness of structural element
w	width of structural element
σ_u	tensile strength as measured conventionally ("smooth" specimen)
σ_u'	local tensile strength at tip of crack
σ_y	yield strength (0.2 percent offset)

Subscript:

eq	equivalent

THROUGH CRACKS IN PLANE TENSILE ELEMENTS

The Method of Crack-Strength Analysis

The specimen geometries considered are shown in sketch (a). The length of the element is assumed to be sufficiently large to make length effects negligible. The length of the crack is measured before loading begins. The load is assumed to increase monotonically, and the failing or ultimate load is defined as the maximum load carried before or at complete failure.

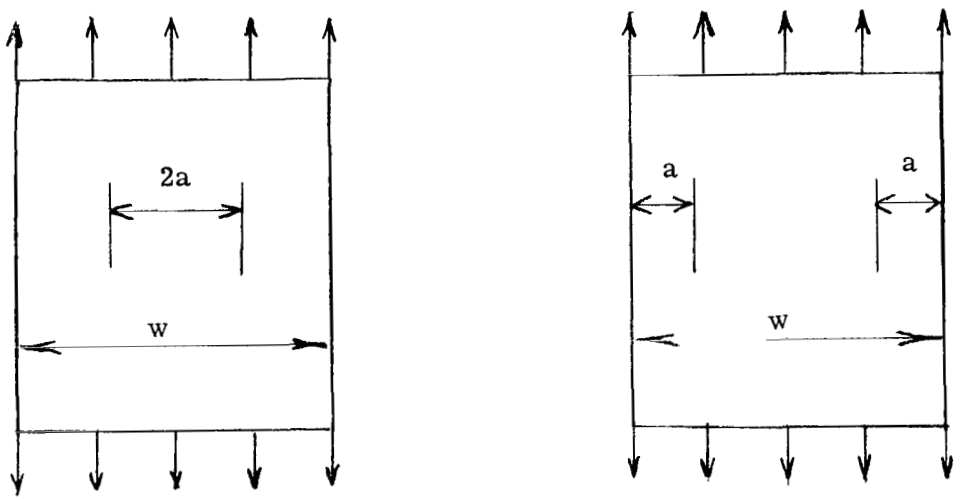

Sketch (a)

The stress at the tip of the crack ("peak stress") is a uniaxial tensile stress parallel to the applied stress but intensified. If it is postulated that the ultimate load is reached when the peak stress becomes equal to the tensile strength σ_u, the net-section stress at failure can be defined by the expression

$$S_N = \frac{\sigma_u}{K_u} \tag{1}$$

According to the method of crack-strength analysis (refs. 1 and 2), the stress-concentration factor K_u is given by the expression

$$K_u = 1 + C_m k_w \sqrt{a} \tag{2}$$

where C_m is a materials constant with the dimension (length)$^{-1/2}$, and k_w is given by the expressions

$$k_w = \sqrt{\frac{1 - \frac{2a}{w}}{1 + \frac{2a}{w}}} \qquad \text{(center crack, (a) in sketch (a))} \qquad (3a)$$

$$k_w = 1 - \frac{2a}{w} \qquad \text{(edge crack, (b) in sketch (a))} \qquad (3b)$$

The quantity C_m is a "constant" only in the same limited sense that tensile strength is a constant, that is, it varies with test temperature, material thickness, and loading rate, and it may be affected by the environment.

It is well known that a circular-section tensile specimen with a sharp circumferential notch can exhibit a tensile strength (average stress on the net section) very much greater than the tensile strength measured on a smooth specimen. The "notch-strengthening" effect is much smaller on specimens with rectangular cross section, but nevertheless is often significant. When it is sufficiently large to be taken into account, expression (1) is written in the more general form

$$S_N = \frac{\sigma_u'}{K_u'} \qquad (4)$$

where σ_u' is the local tensile strength at the tip of a crack, and K_u' is the associated factor of stress concentration. Expression (2) is then correspondingly written in the form

$$K_u' = 1 + C_m' k_w \sqrt{a} \qquad (5)$$

The local tensile strength σ_u' cannot be measured directly; it must be determined indirectly and jointly with C_m'. Thus, a minimum of two tests on cracked specimens is necessary; obviously, the specimens must differ sufficiently in effective crack length $2k_w^2 a$ to afford adequate accuracy in the simultaneous solution of two equations. If it is known or assumed that there is no notch-strengthening $(\sigma_u' = \sigma_u)$, one of the two tests is replaced by a conventional smooth-specimen tensile test to determine σ_u.

Special attention is called to the stipulation that all formulas given should be considered as applicable only if buckling near the crack is prevented or is definitely negligible. A discussion of this buckling effect is given in reference 1.

Correlations of Tests on Sheet Materials

In order to assess the accuracy of correlation achievable by formulas (1) and (2), or (4) and (5), it would be desirable to have some comprehensive sets of test data fulfilling the following requirements:

(a) The width w of the specimens should vary from the minimum used in testing (about 1 inch (2.5 cm)) to the maximum used (currently about 50 inches (127 cm))

(b) For each width, the possible range of crack lengths should be covered by an adequate number of tests

(c) All the material should be from one batch

(d) The material test data should exhibit low scatter.

No known test series fulfills all these requirements entirely, but the series shown in figures 1 and 2 come sufficiently close to serve the purpose.

Figure 1, taken from reference 1, shows results for an aluminum alloy tested at room temperature. In figure 1(a), the curves are computed by the C_m procedure, C_m being chosen to give a good fit at the largest width. (The reason for fitting in this manner becomes evident from the discussion in the section "Use of C_m as Approximation for C_m'.")

The group of points on the extreme right falls below the curves. It is believed that this disagreement can be attributed to the specimen guide plates having had insufficient stiffness to cope with the large buckling forces developed in the presence of these extremely long cracks. For this reason, and because the ratios $2a/w$ involved are well beyond the range of practical interest, these points are disregarded when the accuracy of strength prediction is being assessed.

In the main group of points, the agreement between test points and curves deteriorates somewhat as the width decreases. The maximum discrepancy (at the smallest width) is 11 percent.

Figure 1(b) shows the same set of test points with curves now calculated by the C_m' procedure. If the tests with extreme values of $2a/w$ are again disregarded, it will be seen that the fit is now equally good for the large widths and for the small widths. The remaining errors (at $w = 12$ and 18 inches) alternate in sign and can thus be attributed to scatter. The largest error is now 7 percent, which is less than the difference between two nominally identical specimens at $2a/w = 0.75$.

Figure 2, with test data from reference 4, shows results for another aluminum alloy tested at cryogenic temperature. Figure 2(a) shows results for specimens with longitudinal grain; figure 2(b), results for specimens with transverse grain. The curves are computed by the C_m' procedure. The maximum discrepancy between a test point and the relevant curve is 3.5 percent for figure 2(a) and 6 percent for figure 2(b).

From figures 1 and 2 it is evident that the C_m procedure is capable of correlating fracture data for aluminum alloys. Correspondingly comprehensive sets of tests on materials other than aluminum alloys are not known. However, a large number of

test sets on many different materials has been examined, and most of these sets could be fitted well or at least reasonably well. Some of this test evidence is presented in reference 1.

Use of C_m as Approximation for C_m'

The determination of the constants C_m' and σ_u' requires, as pointed out in the section "The Method of Crack Strength Analysis," tests at widely different effective crack lengths $2k_w^2a$. At present, available data, particularly for thick sections, are often confined to a single value of crack length or to a very narrow range; thus, it is possible only to determine a value of C_m. Strength predictions based on such a value of C_m are approximations if the material exhibits notch strengthening, that is, if the use of C_m' is necessary to characterize the crack strength accurately. It is of practical interest to examine the consequences of such an approximation.

Constants of an actual material as given in figure 2(b) were used to furnish a numerical example $\left(C_m' = 3.75 \text{ inches}^{-1/2} \ (2.35 \text{ cm}^{-1/2}); \ \sigma_u'/\sigma_u = 1.44\right)$. With these constants, the normalized crack strength was computed as a function of the parameter $k_w\sqrt{a}$ and is shown in figure 3 as the solid-line curve.

Assume now that the investigator has available only one test made with configuration A. This configuration has $k_w\sqrt{a} = 0.3 \text{ inch}^{1/2} \ (0.48 \text{ cm}^{1/2})$, which might be realized, for instance, in a specimen with $w = 1.12$ inches (2.84 cm) and $2a/w = 0.33$. Configuration A gives $C_m = 1.59 \text{ inches}^{-1/2} \ (1.00 \text{ cm}^{-1/2})$, and the crack strength calculated with this value of C_m is shown as the upper dashed curve in figure 3. To the left of point A, the dashed curve is a conservative approximation to the solid-line curve. All curves are arbitrarily terminated at $k_w\sqrt{a} = 0.1 \text{ inch}^{1/2}$; at this point, approximation A is about 18 percent conservative. To the right of point A, that is, for effective crack lengths greater than those for configuration A, the approximation is unconservative; at the right-hand end of the curves, the approximation overestimates the crack strength by about 47 percent. If "useful accuracy" is defined arbitrarily as ±20 percent, it may be seen that approximation A has useful accuracy only for $k_w\sqrt{a} < 0.8 \text{ inch}^{1/2} \ (1.3 \text{ cm}^{1/2})$.

Assume that the investigator is given the test result for configuration B, with $k_w\sqrt{a} = 2.0 \text{ inches}^{1/2} \ (3.2 \text{ cm}^{1/2})$. This configuration gives $C_m = 2.45 \text{ inches}^{-1/2} \ (1.54 \text{ cm}^{-1/2})$, and the approximate strength calculated with this value is shown as the lower dashed curve in figure 3. Again, the approximation is conservative to the left of the "comparison point" B, and unconservative to the right of point B. However, the maximum unconservatism is now so small that it does not show in the figure, and useful accuracy exists over almost the entire length of the curve.

In any given material, the crack lengths of potential practical interest range from very small values to rather large ones. Ideally, tests should cover this range in order to

permit the determination of the two constants C_m' and σ_u'. If this is not feasible, the effective crack length for the test should be chosen as large as feasible in order to minimize prediction errors, particularly for unconservative predictions, when the entire range of practical interest is considered.

Example of Thickness Effect

Figure 4, taken from reference 1, shows a plot of C_m against thickness for an aluminum alloy. It is seen that C_m increases markedly with increasing thickness, and the curve for transverse grain is still sloping upward at the largest thickness.

SURFACE CRACKS IN PLANE TENSILE ELEMENTS

Method of Calculation

Service experiences have evoked a growing interest in surface or "part-through" cracks, and a large amount of testing has been done with such cracks in the past few years. It would be very useful, therefore, if the method of strength analysis for through cracks presented in the preceding sections could be extended in order to provide a corresponding capability of strength prediction for surface cracks. A formula for this purpose has been chosen on the basis of the following considerations.

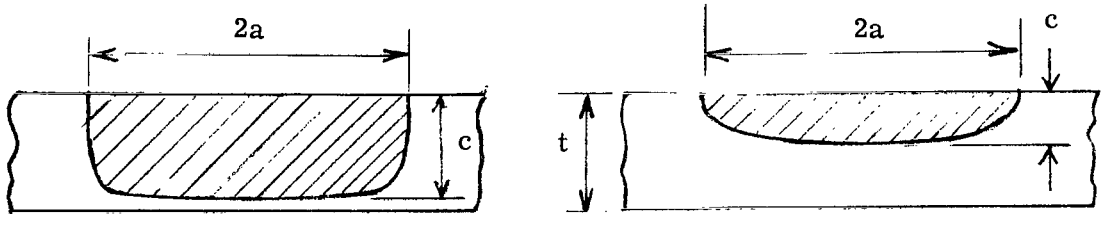

(a) (b)

Sketch (b)

A surface crack, with a length $2a$ measured on the surface ((a) part of sketch (b)), can be replaced formally (as far as effect on strength is concerned) by a through crack having an "equivalent length"

$$2a_{eq} = 2aF$$

where F is a correction function. For a crack of approximately rectangular shape, such as shown in (a) part of sketch (b), it is clear that F approaches 1.0 as c approaches t (a nearly through crack). In the opposite limiting case of a scratch (c approaches 0), it is clear that F approaches 0 because a surface scratch of vanishing depth has no effect on the strength. The simplest function F which fulfills the two limiting conditions is $F = c/t$. However, after a preliminary analysis, the function $F = (c/t)^2$ was tentatively chosen. Since the area of a rectangular crack is $A_c = 2ac$, the tentative formula for the equivalent crack length may be written in the form

$$2a_{eq} = A_c \frac{c}{t^2} \tag{6}$$

In practically all the tests to be presented, surface flaws were produced by first generating an initial flaw (usually by electrical-discharge machining) and then subjecting the specimen to bending fatigue. The resulting fatigue crack is generally a rather good approximation to a semiellipse, the horizontal half-length a being greater than the depth c ((b) part of sketch (b)). Formula (6) was tentatively assumed to be applicable to such shapes (with $A_c = \pi ac/2$), and the experimental evidence presented later indicates that the formula may be considered as sufficiently accurate for use in design. As noted, practically all the experimental evidence is obtained from cracks of such semielliptical shapes; some experimental data on other crack shapes appear among the data discussed in appendix B, but the data are too limited in scope and show too much scatter to lead to useful conclusions. It is suggested, therefore, that caution be used in applying formula (6) to shapes not resembling that shown in (b) part of sketch (b), at least in crack-sensitive materials.

Correlations Between Through Cracks and Surface Cracks

The experimental evidence presented in figures 5 to 14 consists of 25 sets of tests on tensile specimens with surface cracks. For each set, there is at least one through-crack test made on a specimen of the same material as part of the set.

For each surface-crack specimen, the equivalent crack length was computed by expression (6); the crack shape was assumed to be a semiellipse for the purpose of computing the crack area. The net-section stress at failure, in the nondimensional form S_N/σ_u, was then plotted against the equivalent crack length. Average values or ranges of the ratio crack depth to crack length c/2a and of the ratio crack depth to sheet (or plate) thickness c/t are shown in each of the figures.

From the through-crack test (or tests) and the coupon value of σ_u, the value of C_m was computed for each set. With this value of C_m, the curve of $S_N/\sigma_u \left(= 1/K_u\right)$ was computed and plotted as a solid-line curve. The solid-line curves thus constitute predictions for the test points representing surface cracks and contain no adjustments based on

these test points. In most cases, only a single test was available to determine C_m; thus, detailed studies of the accuracy of prediction are not justified.

A number of test sets contained specimens of different widths. Where feasible, the computed curves are shown in two or more segments, each segment being computed for the appropriate width. For example, in figure 6(b), the left-hand segment of the curve is computed with $w = 7$ in. (18 cm), which is the average value of w for the specimens denoted by diamond-shaped, circular, and triangular symbols, whereas the right-hand segment is computed with $w = 12$ in. (30 cm), the value of w for the specimens denoted by square symbols. Where test points for different widths were intermingled, the computation was based on the average width for the test group. This procedure was considered to be sufficiently accurate, because the effect of changes of width was relatively small when compared with that for test scatter.

For five of the test sets, additional curves were computed, shown as dashed lines. These curves are computed by the C_m' procedure in such a manner as to obtain a perfect fit for the through-crack test and the best fit obtainable for the surface-crack tests. Other details are explained in the individual discussions.

Test data available at present for thick sections (thick sheet and plate) are, with negligible exceptions, too limited in scope to permit the use of the C_m' procedure. As discussed in the section "Use of C_m as Approximation for C_m'," the use of C_m instead of C_m' should tend to result in conservative strength predictions as long as the crack length with which C_m was determined is larger than the crack lengths for which predictions are made. For each test set shown, the crack length and specimen width of the through-crack specimen used to determined C_m is given, and it may be seen that the length of the through crack was always substantially larger than the largest value of $2a_{eq}$.

Tests on 2219-T87 aluminum alloy.- Tests on this alloy, made for two thicknesses (sheet and plate) and at three test temperatures, are taken from reference 5 and are shown in figures 5, 6(a), 6(b), and 6(c). In most cases, only a single computed curve based on the average width of specimen is shown; use of this single curve is sufficiently accurate to appraise the accuracy of the predictions. It may be seen that the predictions tend to be conservative. Figures 6(d), 6(e), and 6(f) show additional sets of tests made on the thick-plate material. They are shown separately from the previous tests (figs. 6(a) to 6(c)) for two reasons: the specimens are large and contain large cracks, and their plots require a longer abscissa scale; more importantly, the material exhibited a number of cases of delamination at the crack tips. Specimens for which delamination was reported are denoted by solid symbols. The figures are discussed most conveniently in reverse order.

For tests at -423° F (20 K), as shown in figure 6(f), no delaminations were reported, and all tests points are close to the predicted curve. At -320° F (77 K), one case of delamination was reported, as shown in figure 6(e), and the test stress lies very substantially above the curve, whereas the nine tests without delamination lie reasonably close to the curve. The high value of the failing stress for the delaminated specimen agrees qualitatively with the observation that laminated plates produced by gluing together several layers of sheet display the high crack resistance characteristic of the sheet.

At room temperature, delamination was reported for four specimens as shown in figure 6(d). For the largest cracks, the effect of delamination was apparently mainly a widening of the scatter range. In the group of the four smallest cracks, three show phenomenally high values of stress. Only for one of these three was delamination reported. It should be remarked, however, that the test report used as reference was a preliminary report; it is possible, therefore, that the other two specimens simply had not yet been examined at the time of reporting.

Obviously, values of C_m obtained from delaminating specimens should not be used for design calculations.

Tests on Ti-5Al-2.5Sn alloy.- This alloy was tested in two thicknesses and at three temperatures (ref. 5); the results are shown in figures 7 and 8.

For the thick material with $t = 0.20$ inch (5 mm), the agreement between the test points and the curves computed by the C_m procedure is reasonably adequate, as shown in figure 7. For the thin material with $t = 0.020$ inch (0.5 mm), on the other hand, the agreement with the C_m predictions is generally poor (fig. 8), and a discussion of each test set is required.

For the test set at -423° F (20 K) shown in figure 8(d), all test points lie above the solid-line curve computed by the C_m procedure; the trend suggests that notch strengthening is operative here. By a trial-and-error procedure, the ratio $\sigma_u'/\sigma_u = 1.4$ was selected. The through-crack test then gives a value of C_m' as shown in the figure, and the dashed-line curve calculated with this value of C_m' gives a satisfactory fit along the lower edge of the scatter band.

Figures 8(a), 8(b), and 8(c) include a "cut-off line" (marked in fig. 10(b)). This line gives the net-section stress that would exist if the stress on the gross section became equal to σ_u, the specimen consequently failing at some section away from the crack. The equation of the cut-off line is

$$\frac{S_N}{\sigma_u} = \frac{1}{1 - 2a/w}$$

Figure 8(b) shows the first evaluation of the test results at -320° F (77 K), all computations being based on the reported coupon value of σ_u. It will be seen that ten test points

lie above the cut-off line. There is only one possible explanation for such a result: The reported coupon value of σ_u is not representative of these test specimens.

The point representing four specimens on the left in figure 8(b) is 5.3 percent above the cut-off line. It was assumed, therefore, that the actual tensile strength was 5.3 percent higher than the reported coupon value, and a new plot was made as shown in figure 8(c). All test points have been shifted down 5.3 percent, the value of C_m has been recomputed from the through-crack test, and a new prediction curve has been computed. The agreement is now satisfactory. (Note that no notch strengthening was assumed.)

At room temperature, only two tests were made as shown in figure 8(a); the average of the two tests lie on the cut-off line. The prediction by the C_m procedure, which implies no notch strengthening, is very conservative. The prediction by the C_m' procedure, if the notch-strengthening ratio σ_u'/σ_u is assumed to be the same as that for figure 8(d), agrees well with the average of the two test points.

The various assumptions that had to be made in order to arrive at the final results shown in figure 8 suggest that the crack-sensitivity constants derived should be regarded with considerable caution. However, a general observation based on a comparison between figures 7 and 8 is believed to be worth noting.

Figure 7 shows that the thick material is remarkably insensitive to cracks at room temperature. At -320° F (77 K), however, a drastic increase in sensitivity is shown, and only a rather small additional increase is shown when the temperature is further decreased to -423° F (20 K). The thinner material (fig. 8), on the other hand, retains the low crack sensitivity shown at room temperature down to -320° F; when the temperature is decreased further to -423° F, the crack sensitivity increases markedly although it is still considerably less than that for the thicker material at the same temperature. From the data shown, it would be impossible to predict with any degree of confidence whether a sheet of a thickness intermediate between the two test values would be very "tough" or very "brittle" at -320° F (77 K). Thus, verification tests and additional tests are obviously necessary to define the crack sensitivity adequately.

Tests on 300 M steel.- The tests on 300 M steel reported in reference 6 introduce a parameter not involved in the tests previously discussed: the presence of hostile environments (moist air or salt spray). A very large scatter is evident in figures 9 and 10; consequently, the through-crack tests were also made in fairly large numbers.

The original investigators concluded that the two environments produced essentially the same results. Examination of the original data showed no reason to disagree with this conclusion; consequently, the through-crack data for the two environments were pooled for the determination of C_m. On the plots for the surface-crack specimens (figs. 9 and 10), the data are also pooled, but different symbols are used for the two

environments. The agreement between test points and curves is about as good as can be expected in view of the large scatter.

In figure 10, it may be seen that the highest crack sensitivity (highest value of C_m) is displayed by the material heat treated to the intermediate strength level. The original investigators (ref. 6) made the same observation, although they used a different method for evaluating the crack sensitivity, and they noted that this observation is contrary to expectation.

Two sets of data presented in appendix B (fig. 15) on the same type of material but tested in the normal laboratory environment show remarkably smooth curves; thus, the large scatter evidenced in figures 9 and 10 and in the accompanying through-crack data should presumably be attributed entirely to the hostile environment.

Tests on various materials.- Nine test series were available on various materials and are presented in figures 11 to 14. Test data are taken from references 7 and 8. Only a rather small number of tests with surface cracks were made in each case; however, in most cases, two or even three tests were made with through cracks. Thus, good confidence in the value of C_m calculated from them is justified. In one case (fig. 12(a)), it was necessary to obtain C_m by interpolating between two tests made for a smaller and a larger thickness. One case (AM 355, fig. 13(b)) requires some explanation.

Only a single through-crack test was made at -110° F (194 K); the value of C_m obtained from this test resulted in curve A shown in figure 13(b), which is evidently rather low. On the same material, two through-crack tests were made at room temperature, and the failing stresses differed by 20 percent. It was assumed, then, that increasing the failing stress obtained in the single test at -110° F by 10 percent might result in a more representative value of the crack strength and thus of C_m. The curve calculated with this new value of C_m is shown as curve B. Finally, still using the increased value of failing stress, it was assumed that notch strengthening was operative; with a ratio $\sigma_u'/\sigma_u = 1.50$ determined by trial and error and the corresponding value of C_m', curve C resulted. (A plot for AM 355 at room temperature is not shown because only a single test was made with a surface crack.)

With the exception of the tests of AM 355 material discussed, all the test series shown in figures 11 to 14 show satisfactory agreement between the test points and the curves calculated by the C_m procedure.

Discussion of correlations between through cracks and surface cracks.- The data on through cracks for figures 5 to 14 were not adequate to determine values of C_m' (and σ_u'); consequently, it was necessary to use C_m in all cases for the first set of strength predictions. For four sets of data (figs. 8(a), 8(d), 13(a), and 13(b)), it was possible to use the surface-crack data in conjunction with the through-crack data to estimate C_m'

and σ_u'. The predictions based on C_m' (dashed lines in figs. 8(a), 8(d), 13(a), and 13(b)) were always better than the predictions based on C_m, although the difference was very small in the case of figure 13(a).

In figures 5 to 14 (excluding the figures just discussed), the predicted strengths are either reasonably close or somewhat conservative unless there are obvious disturbing factors such as a hostile environment or delamination. The accuracy of the predictions is felt to be reasonably adequate for practical use in design, if it is borne in mind that the design value of crack size is chosen on the basis of inspection capability and is thus not very precisely definable.

CONCLUDING REMARKS

The main problem in dealing with residual strength in the presence of cracks may be formulated as follows: Given a sheet (or plate) element containing a transverse crack and subjected to a steadily increasing uniaxial tensile load, how can the failing load be predicted? The present paper proposes some simple engineering answers to this question.

For through-the-thickness cracks, the proposed answer is the method of crack-strength analysis (C_m' method) previously published and reviewed herein. Applications to many materials indicate that the method should be sufficiently accurate for engineering applications.

For surface cracks, the answer proposed herein is a simple interpolation formula, based on the consideration that the strength reduction caused by a surface crack should lie between the limiting values defined by a through crack on the one hand and a scratch on the other hand. Utilizing materials constants derived from tests with through cracks, strength predictions were made for 25 sets of surface cracks on a variety of materials and are presented herein. The accuracy of the predictions is felt to be adequate to justify use of the proposed formula in design calculations.

Some of the test data indicate that hostile environments may cause large scatter, and that delamination near the crack tip may give misleadingly high values of residual strength.

Langley Research Center,
National Aeronautics and Space Administration,
Langley Station, Hampton, Va., June 20, 1969.

APPENDIX A

CONVERSION OF U.S. CUSTOMARY UNITS TO SI UNITS

The International System of Units (SI) was adopted by the Eleventh General Conference on Weights and Measures, Paris, October 1960, in Resolution No. 12 (ref. 3). Conversion factors for the units used herein are given in the following table:

To convert from U.S. Customary Units	Multiply by	To obtain SI units
Length, in.	2.54×10^{-2}	meter (m)
Stress, ksi	6.894757	meganewton/meter^2 (MN/m^2)
Temperature, ^{o}F	$\frac{5}{9}(^{o}F + 459.67)$	degrees Kelvin (K)

Prefixes and symbols to indicate multiples of units are as follows:

Multiple	Prefix	Symbol
10^{-3}	milli	m
10^{-2}	centi	c
10^{3}	kilo	k
10^{6}	mega	M

APPENDIX B

TEST SERIES FOR SURFACE CRACKS ONLY

This appendix presents a number of test series for surface cracks not accompanied by tests on through cracks. The values of C_m used to compute the curves were determined either to fit the largest crack or to produce a fit with a conservative tendency. The curves are thus not predictions, as those shown in the main body of this paper, but are fitted. Nevertheless, the data are felt to be of sufficient interest to warrant their presentation.

Data from reference 6.- Data from appendix B of reference 6 are presented in figures 15 to 17. The data on two batches of 300 M steel with different carbon content (fig. 15) show remarkably low scatter, in spite of the fact that the crack sensitivity is high, particularly for the material with the higher carbon content. These data justify the belief that the large scatter exhibit in the tests of this material discussed in the text should be attributed to the hostile environment rather than to the material.

Data from reference 9.- Figures 18 and 19 give results for a titanium alloy and a steel each with two heat treatments, based on data given by Randall in reference 9 (pp. 88-125). For the titanium alloy, the "high-strength" heat treatment results in a tensile strength only 7 percent higher than the tensile strength for the "low-strength" treatment. The values of C_m, however, differ by a factor of five; thus, it is illustrated once again that tensile strength is a poor index of crack sensitivity.

For the D6-AC steel, the two values of C_m differ by a factor of over ten, but for this material, the difference in tensile strength is large enough to give warning that the crack sensitivity may differ substantially, at least to an engineer somewhat familiar with materials properties.

The four sets of tests by Randall are of special interest because a deliberate effort was made to produce some crack shapes other than the "normal" semiellipse (Randall's terminology) with its major axis on the surface of the specimen. In figures 18 and 19, the results for "nonelliptical" and "irregular" crack shapes are emphasized by using solid symbols. For either material in the less crack-sensitive condition ("low-strength" condition), the solid points lie within the scatter bands for the open points, with the exception of one very low point for a large crack in the steel. For both materials in the crack-sensitive condition, the number of solid points is unfortunately very small; for the steel, three out of the four solid points lie substantially below the scatter band. Taken at face value, this observation suggests that strength estimates made by using the equivalent crack length as defined by expression (6) may be very unconservative for cracks of irregular shape in crack-sensitive materials.

REFERENCES

1. Kuhn, Paul: Residual Strength in the Presence of Fatigue Cracks. AGARD Adv. Rep. 11, 1967.

2. Kuhn, Paul: Strength Calculations for Sheet-Metal Parts With Cracks. Mater. Res. Stand., vol. 8, no. 9, Sept. 1968, pp. 21-26.

3. Comm. on Metric Pract.: ASTM Metric Practice Guide. NBS Handbook 102, U.S. Dept. Com., Mar. 10, 1967.

4. Orange, Thomas W.: Fracture Toughness of Wide 2014-T6 Aluminum Sheet at -320° F. NASA TN D-4017, 1967.

5. Masters, J. N.; Haese, W. P.; and Finger, R. W.: Investigation of Deep Flaws in Thin Walled Tanks. NASA CR-72606, 1969.

6. Pendleberry, S. L.; Simenz, R. F.; and Walker, E. K.: Fracture Toughness and Crack Propagation of 300 M Steel. Tech. Rep. DS-68-1, FAA, Aug. 1968. (Available from DDC as AD 676573.)

7. Anon.: Thick Section Fracture Toughness. Tech. Doc. Rep. No. ML-TDR-64-236, U.S. Air Force, Oct. 1964.

8. Anon.: Maraging Steel Project Review. ASD-TDR-63-262, U.S. Air Force, May 1963. (Available from DDC as AD 408962.)

9. Brown, William F.; and Srawley, John E.: Plane Strain Crack Toughness Testing on High Strength Metallic Materials. Spec. Tech. Publ. No. 410, Amer. Soc. Testing Mater., c.1966.

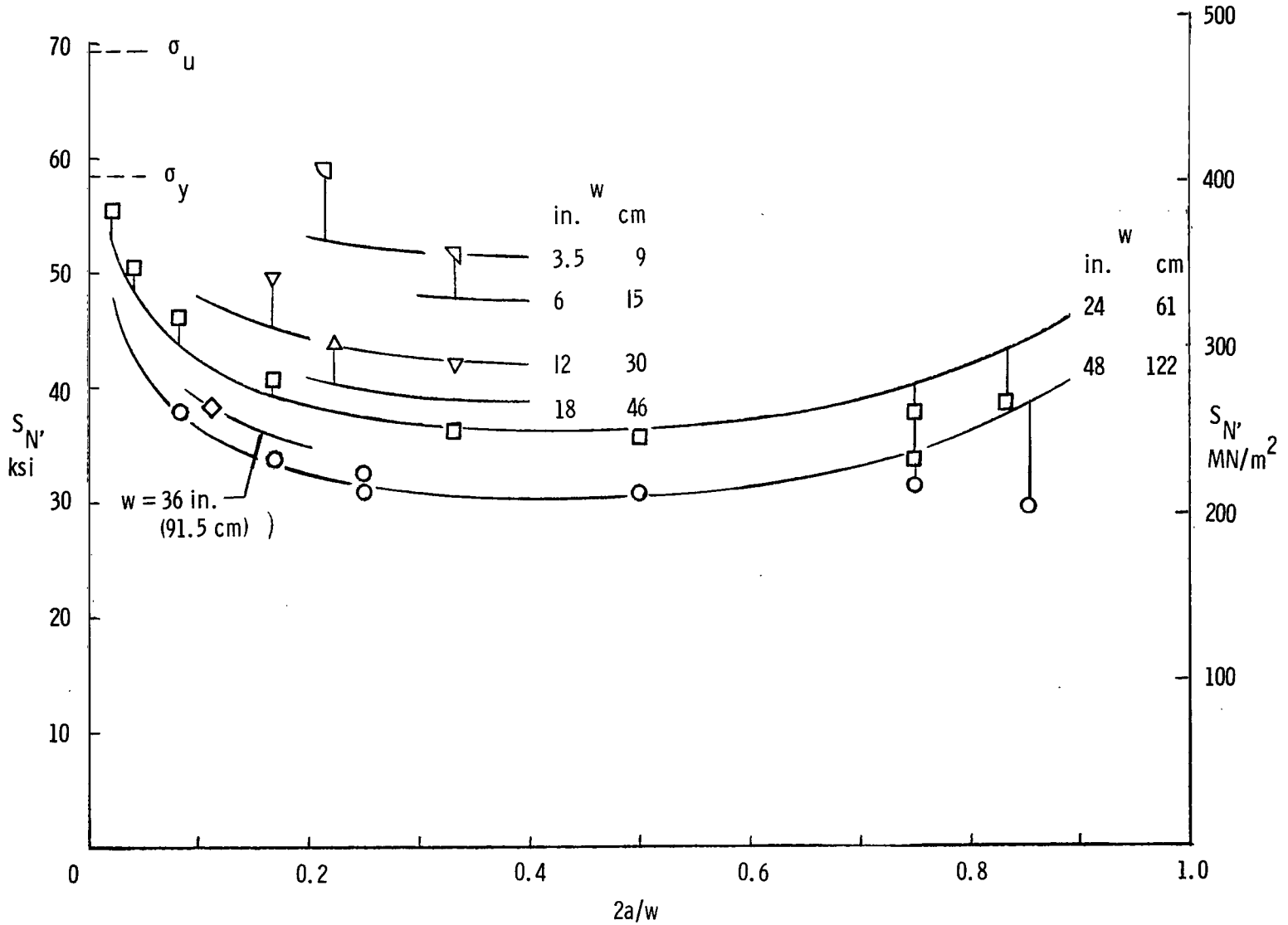

(a) Curves are calculated with $C_m = 0.64$ in$^{-1/2}$ $(0.40$ cm$^{-1/2})$. Figure taken from reference 1.

Figure 1.- Through-crack strength of 2219-T87 sheet, longitudinal grain, at room temperature. Tests by Boeing Aircraft Co. t = 0.1 in. (2.5 mm); $\sigma_u = 69.4$ ksi $(478$ MN/m$^2)$; guides used.

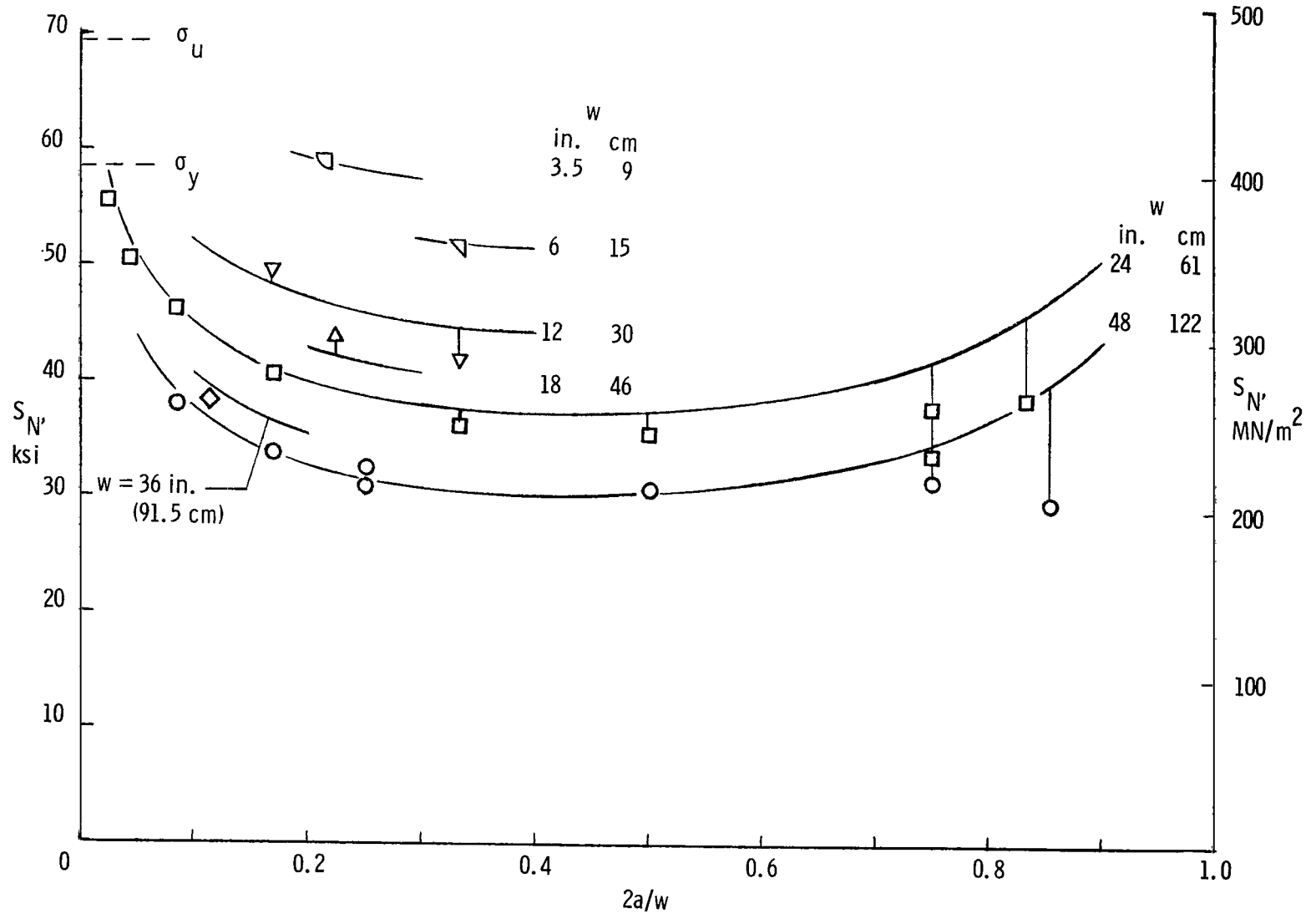

(b) Curves are calculated with $\sigma_u'/\sigma_u = 1.235$; $C_m' = 0.92\ in^{-1/2}\ (0.58\ cm^{-1/2})$. Figure taken from reference 1.

Figure 1.- Concluded.

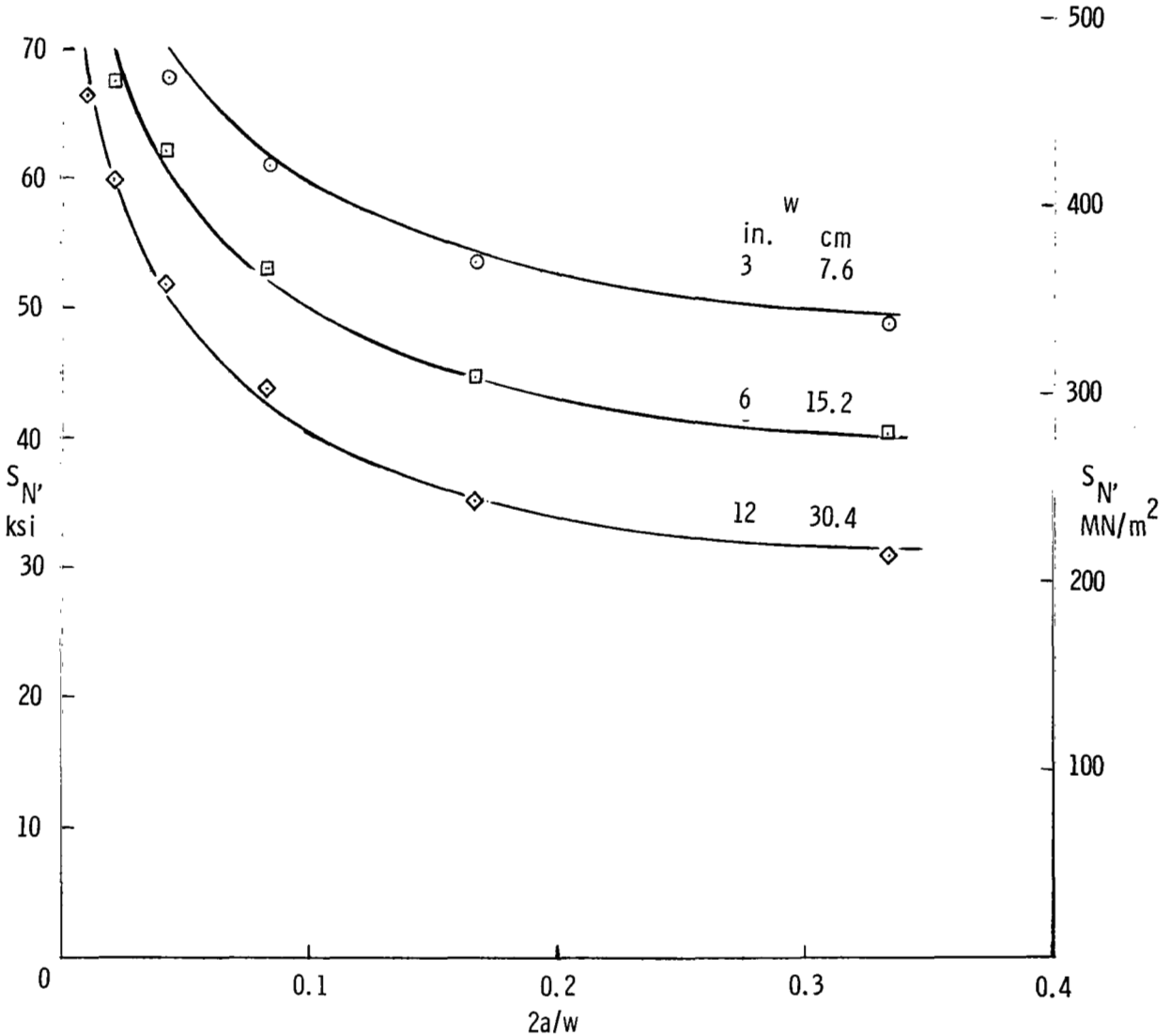

(a) Longitudinal grain; σ_u = 86.6 ksi (597 MN/m^2); σ_y = 75.2 ksi (518 MN/m^2). Curves are calculated with σ_u'/σ_u = 1.330; C_m' = 2.65 in$^{-1/2}$ (1.66 cm$^{-1/2}$).

Figure 2.- Through-crack strength of 2014-T6 sheet at -320° F (77 K). Test data taken from reference 4. Each point is the average of three test points; guides used. t = 0.06 in. (1.5 mm).

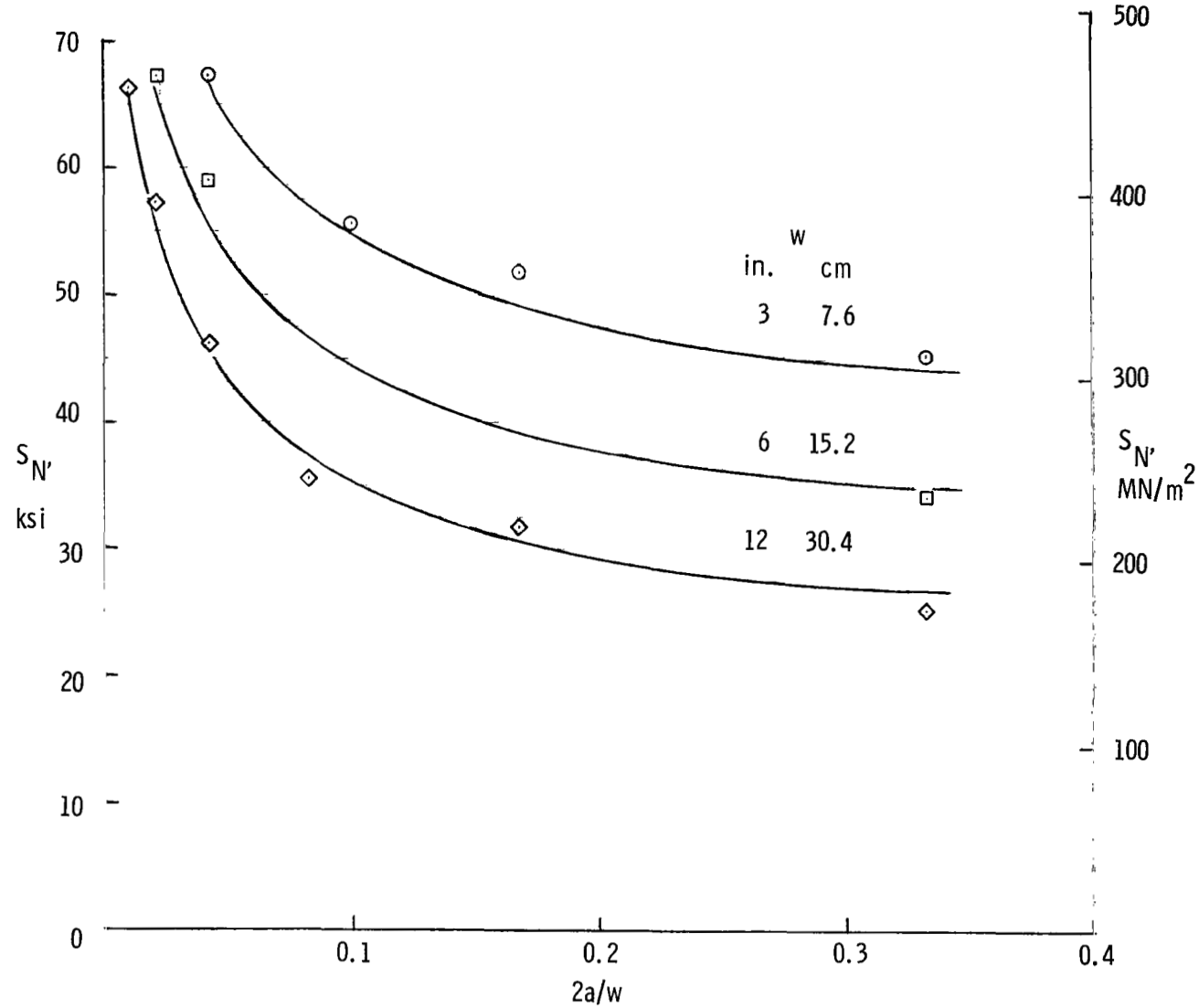

(b) Transverse grain; σ_u = 88.1 ksi (607 MN/m^2); σ_y = 75.9 ksi (523 MN/m^2). Curves are calculated with σ_u'/σ_u = 1.440; C_m' = 3.75 in$^{-1/2}$ (2.35 cm$^{-1/2}$).

Figure 2.- Concluded.

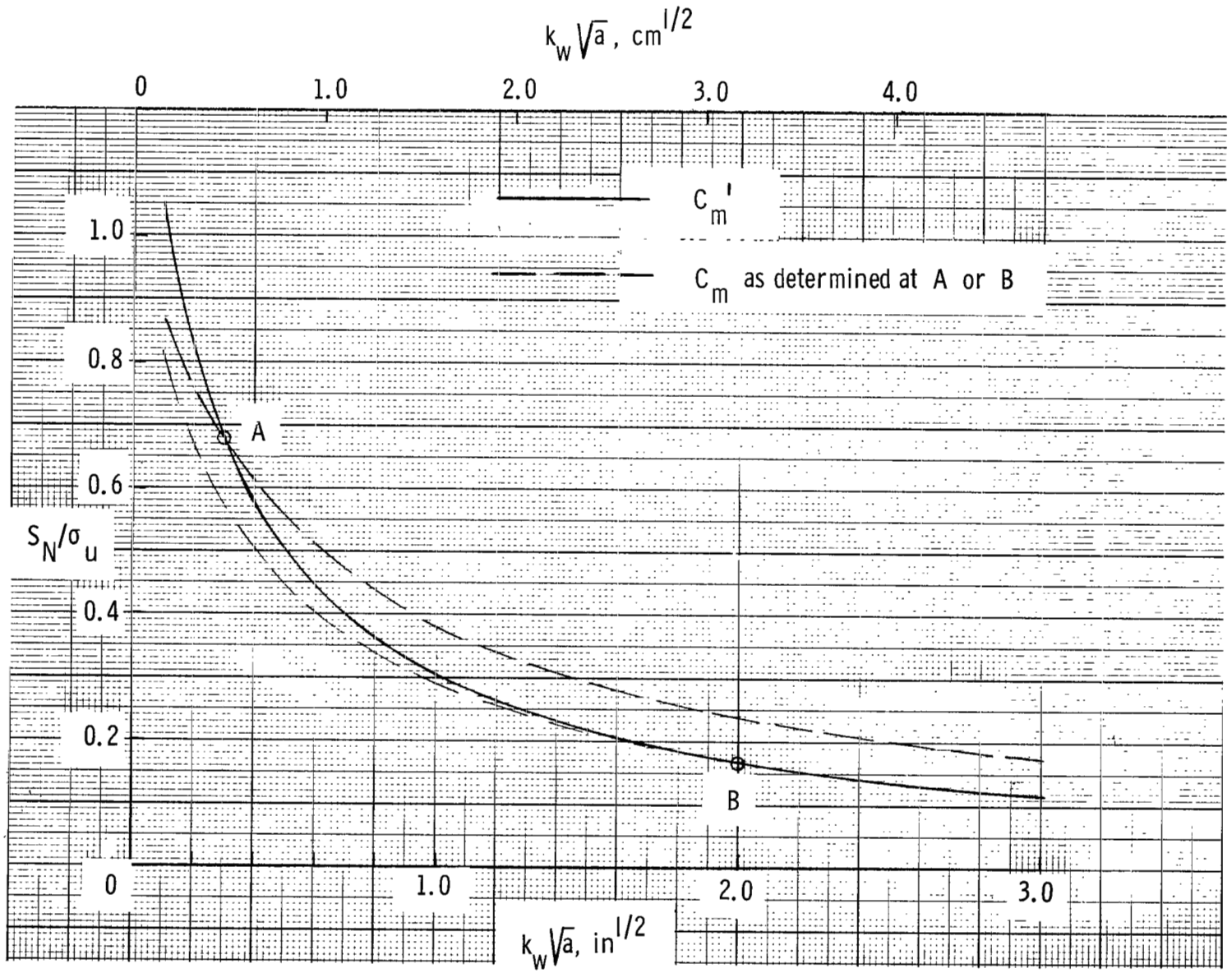

Figure 3.- Effect of using C_m procedure as approximation for C_m' procedure. A and B denote configurations chosen arbitrarily to determine C_m.

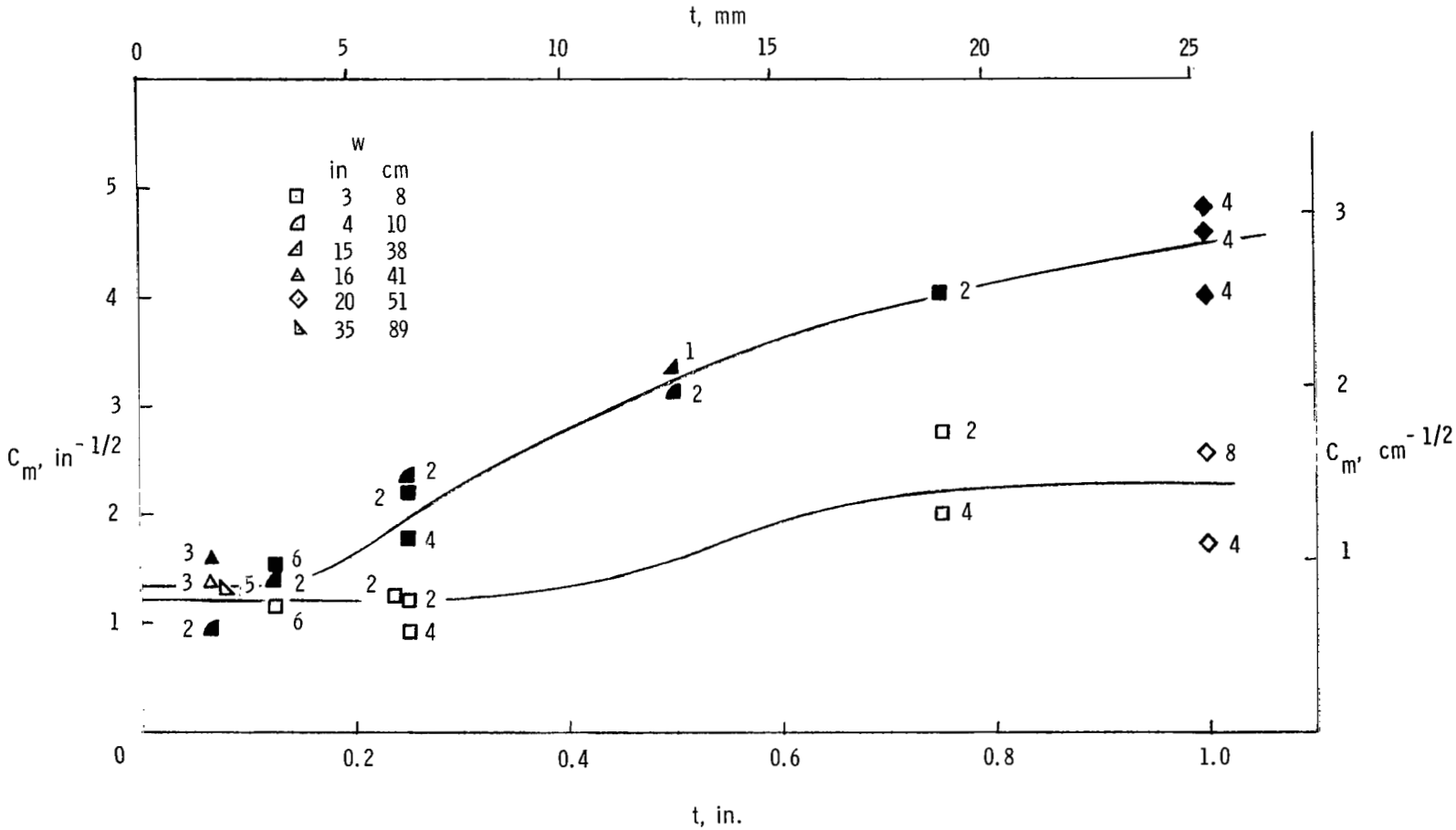

Figure 4.- Variation of C_m with thickness for 7075-T6 or -T651 aluminum alloy. Figure taken from reference 1. Open symbols, long grain; solid symbols, transverse.

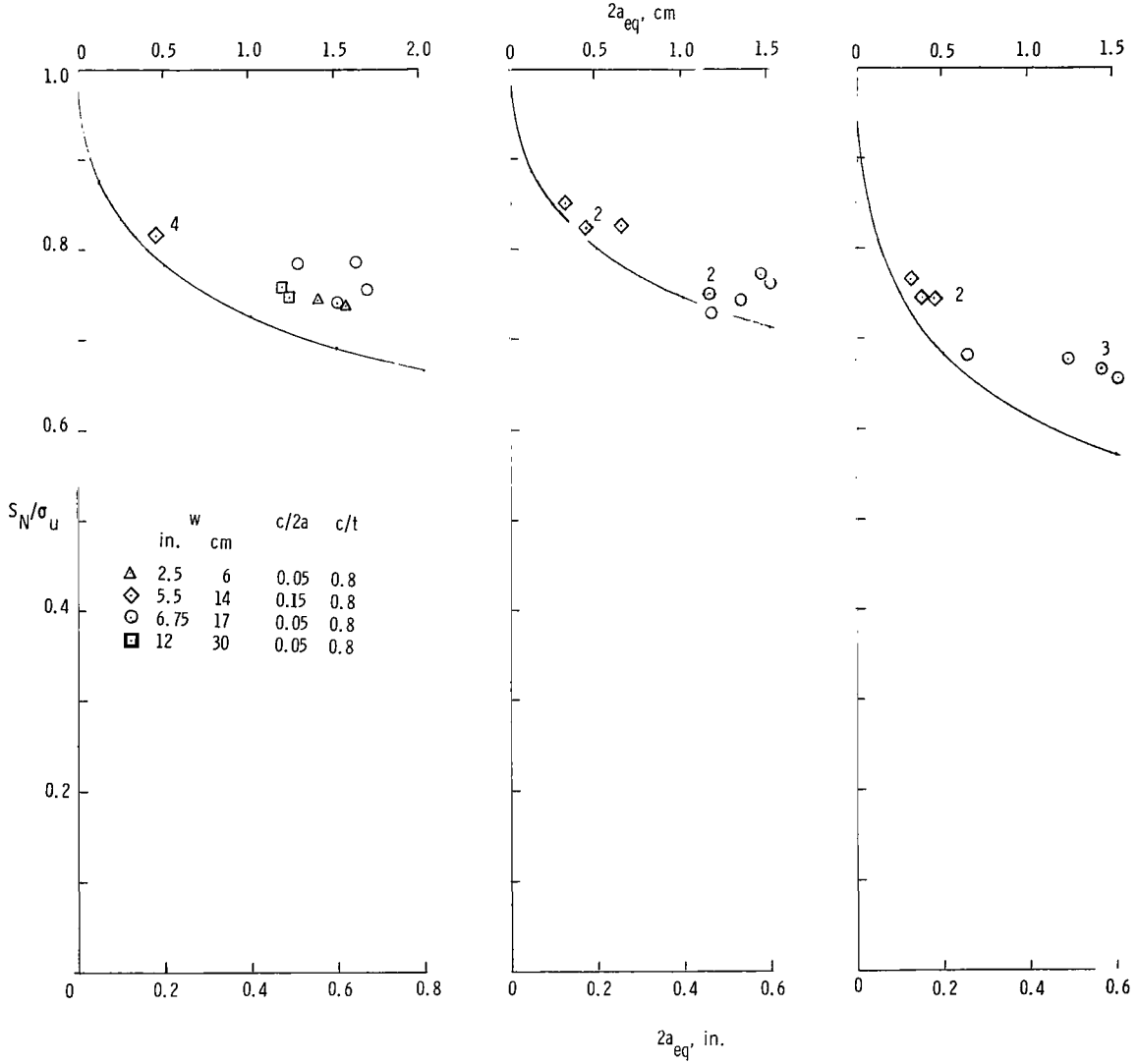

(a) Room temperature; σ_u = 68.0 ksi (469 MN/m^2); curve is calculated with C_m = 0.907 in$^{-1/2}$ (0.569 cm$^{-1/2}$) determined from one through-crack test with 2a = 8 in. (20 cm); w = 16 in. (40 cm).

(b) -320° F (77 K); σ_u = 81.3 ksi (560 MN/m^2); curve is calculated with C_m = 0.820 in$^{-1/2}$ (0.515 cm$^{-1/2}$) determined from one through-crack test with 2a = 8 in. (20 cm); w = 16 in. (40 cm).

(c) -423° F (20 K); σ_u = 95.1 ksi (655 MN/m^2); curve is calculated with C_m = 1.515 in$^{-1/2}$ (0.950 cm$^{-1/2}$) determined from one through-crack test with 2a = 6 in. (15 cm); w = 12 in. (30 cm).

Figure 5.- Surface-crack strength of 2219-T87 aluminum alloy, longitudinal grain, t = 0.06 in. (1.5 mm). Test data taken from reference 5.

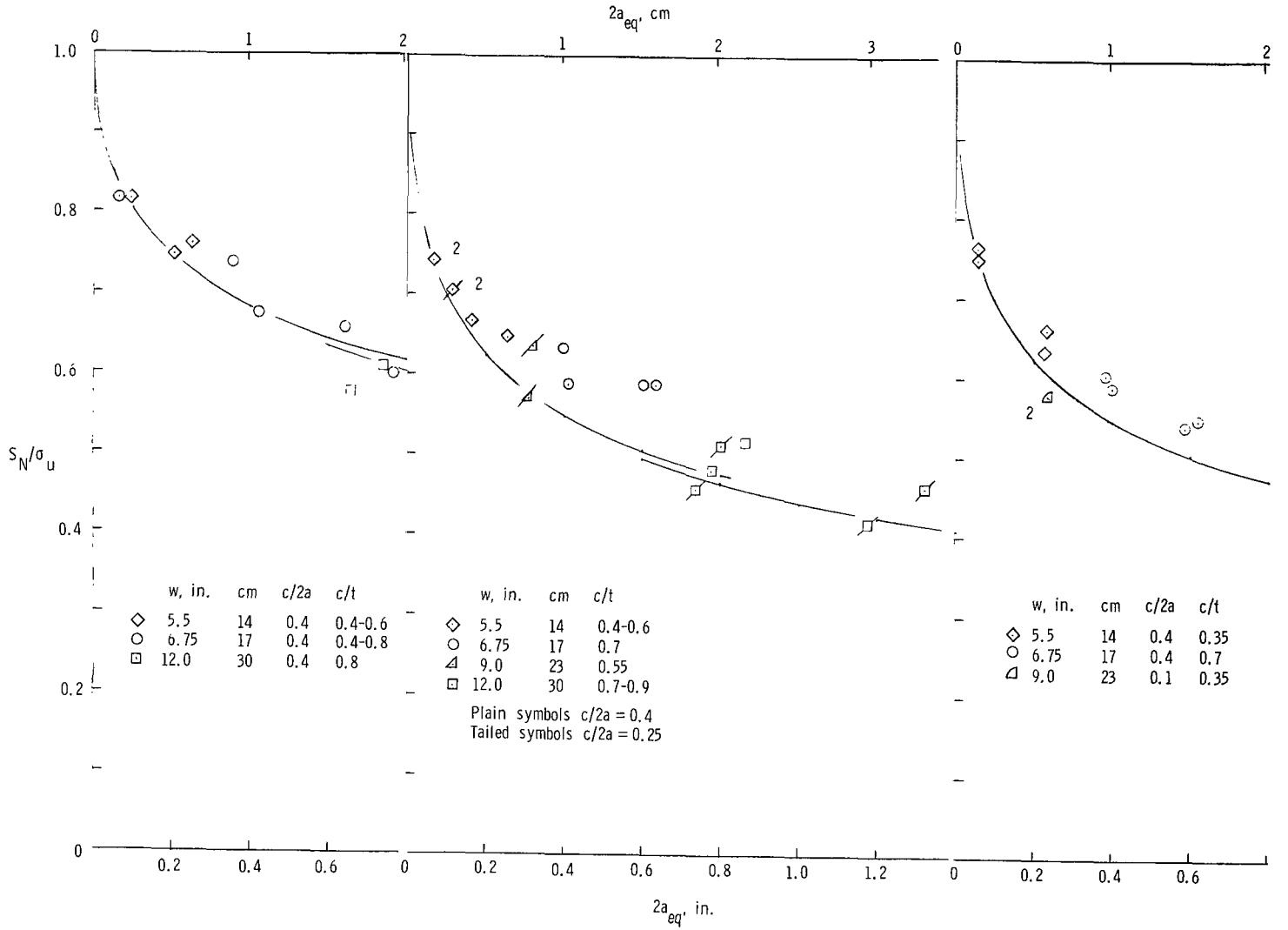

(a) Room temperature; σ_u = 69.3 ksi (477 MN/m^2); C_m = 1.120 in$^{-1/2}$ (0.71 cm$^{-1/2}$) from one through-crack test with 2a = 8 in. (20 cm); w = 16 in. (40 cm).

(b) -320° F (77 K); σ_u = 85.5 ksi (589 MN/m^2); C_m = 1.95 in$^{-1/2}$ (1.226 cm$^{-1/2}$) from one through-crack test with 2a = 8 in. (20 cm); w = 16 in. (40 cm).

(c) -423° F (20 K); σ_u = 92.9 ksi (640 MN/m^2); C_m = 1.977 in$^{-1/2}$ (1.240 cm$^{-1/2}$) from one through-crack test with 2a = 6 in. (15 cm); w = 12 in. (30 cm).

Figure 6.- Surface-crack strength of 2219-T87 aluminum alloy, longitudinal grain, t = 0.63 in. (16 mm). Test data taken from reference 5.

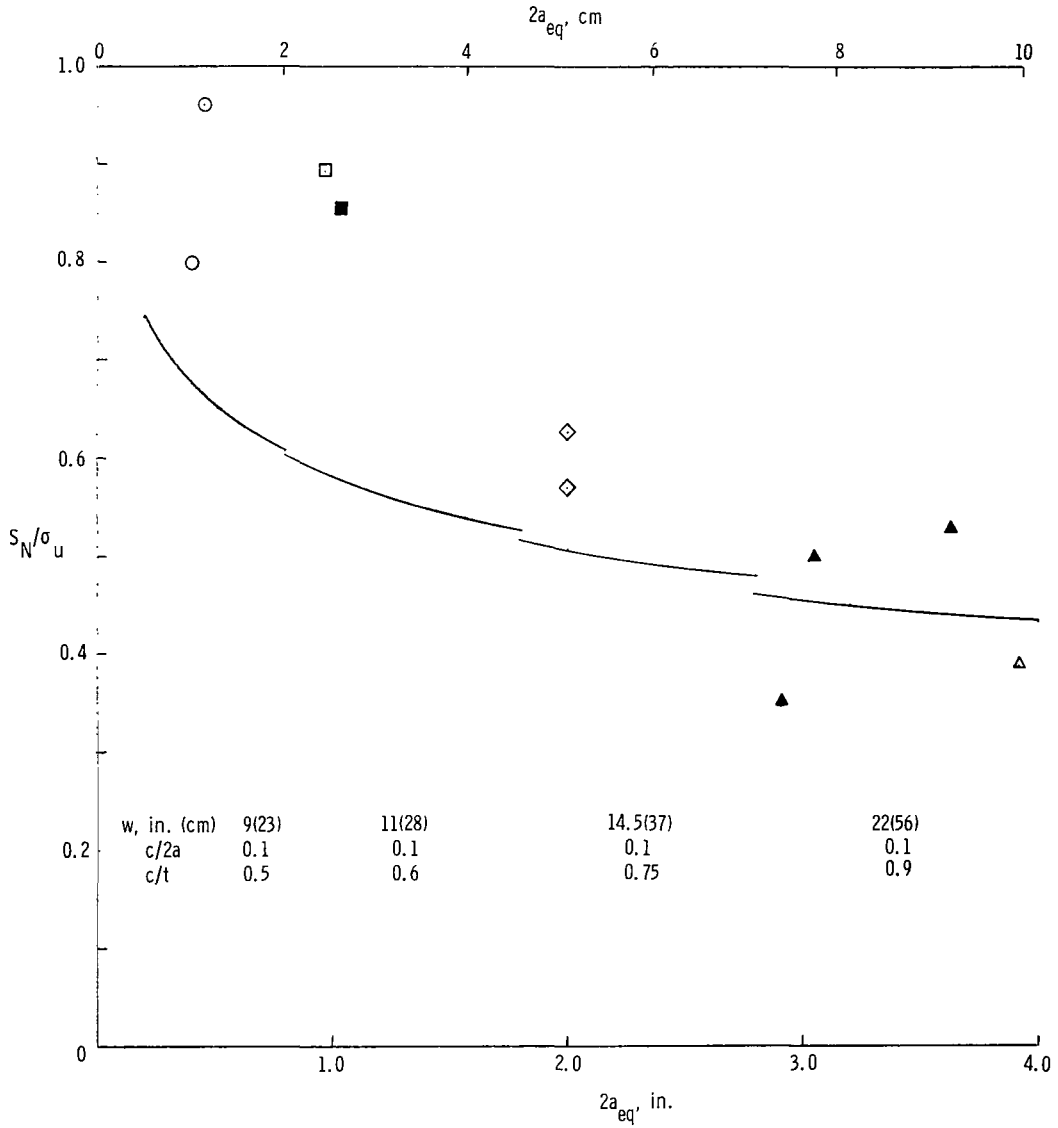

(d) Room temperature; σ_u and C_m same as in figure 6(a); solid points denote specimens in which delamination was observed at crack tips.

Figure 6.- Continued.

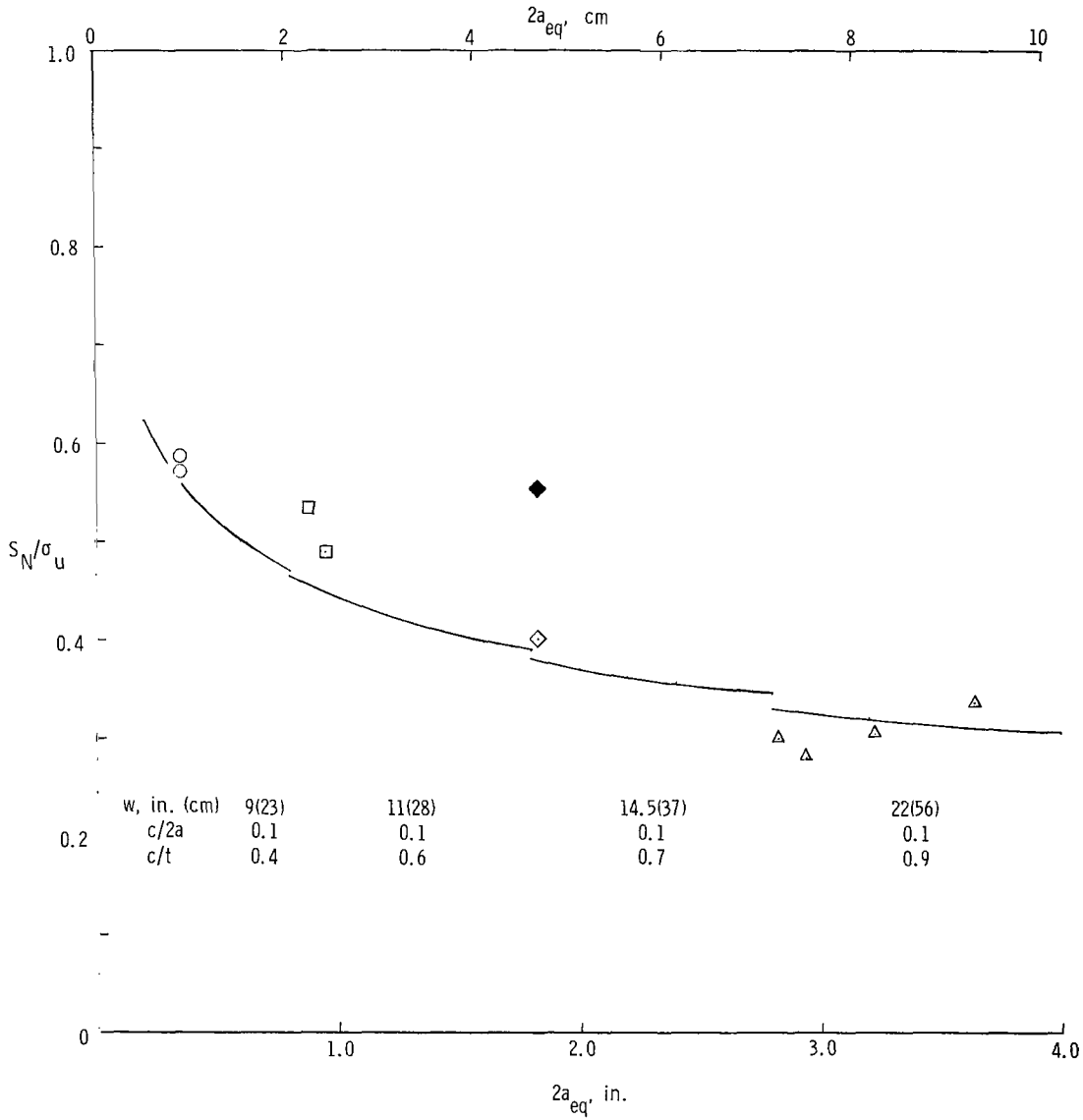

(e) -320° F (77 K); σ_u and C_m same as in figure 6(b); solid point denotes specimen in which delamination was observed at crack tips.

Figure 6.- Continued.

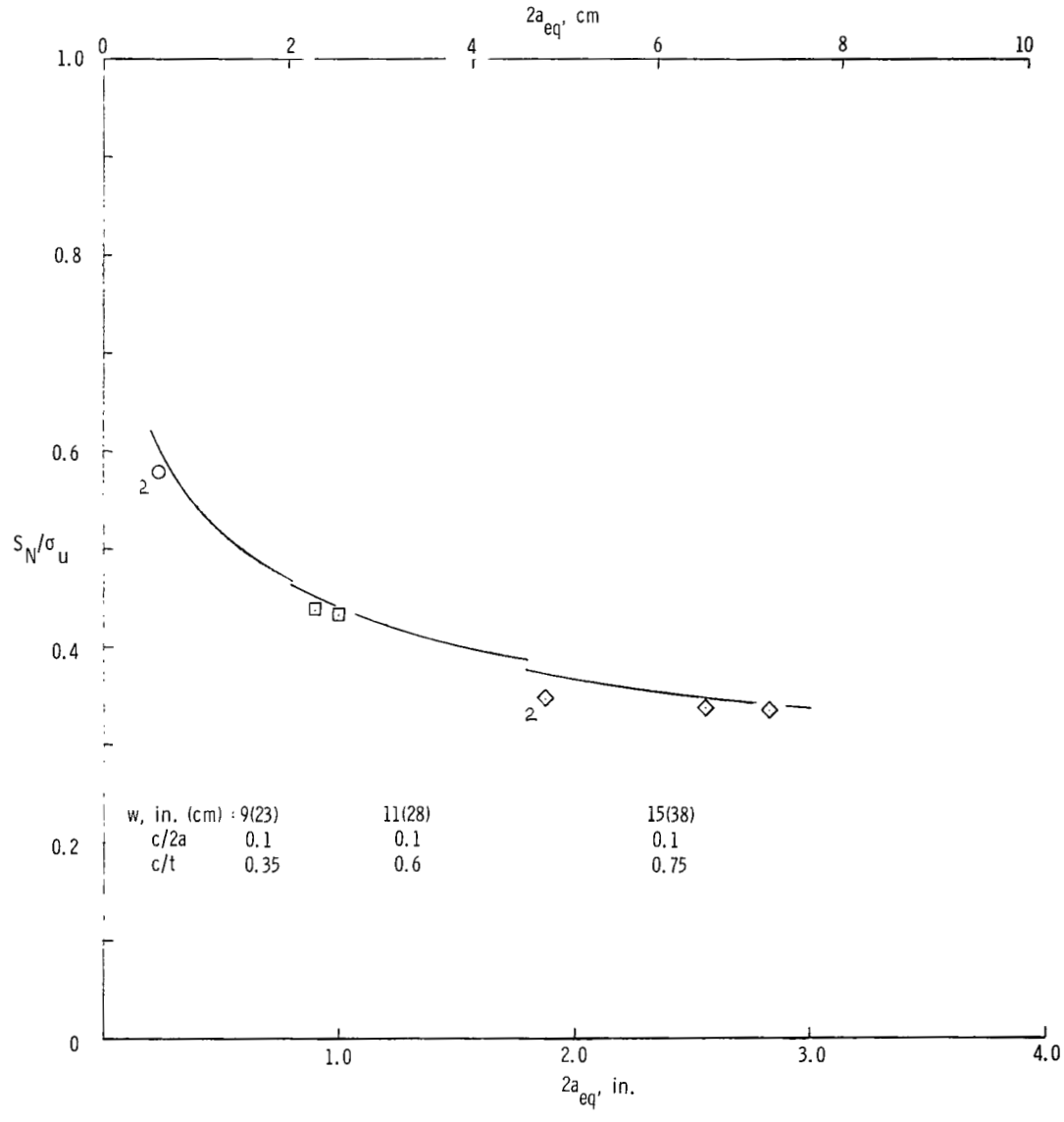

(f) -423° F (20 K); σ_u and C_m same as in figure 6(c).

Figure 6.- Concluded.

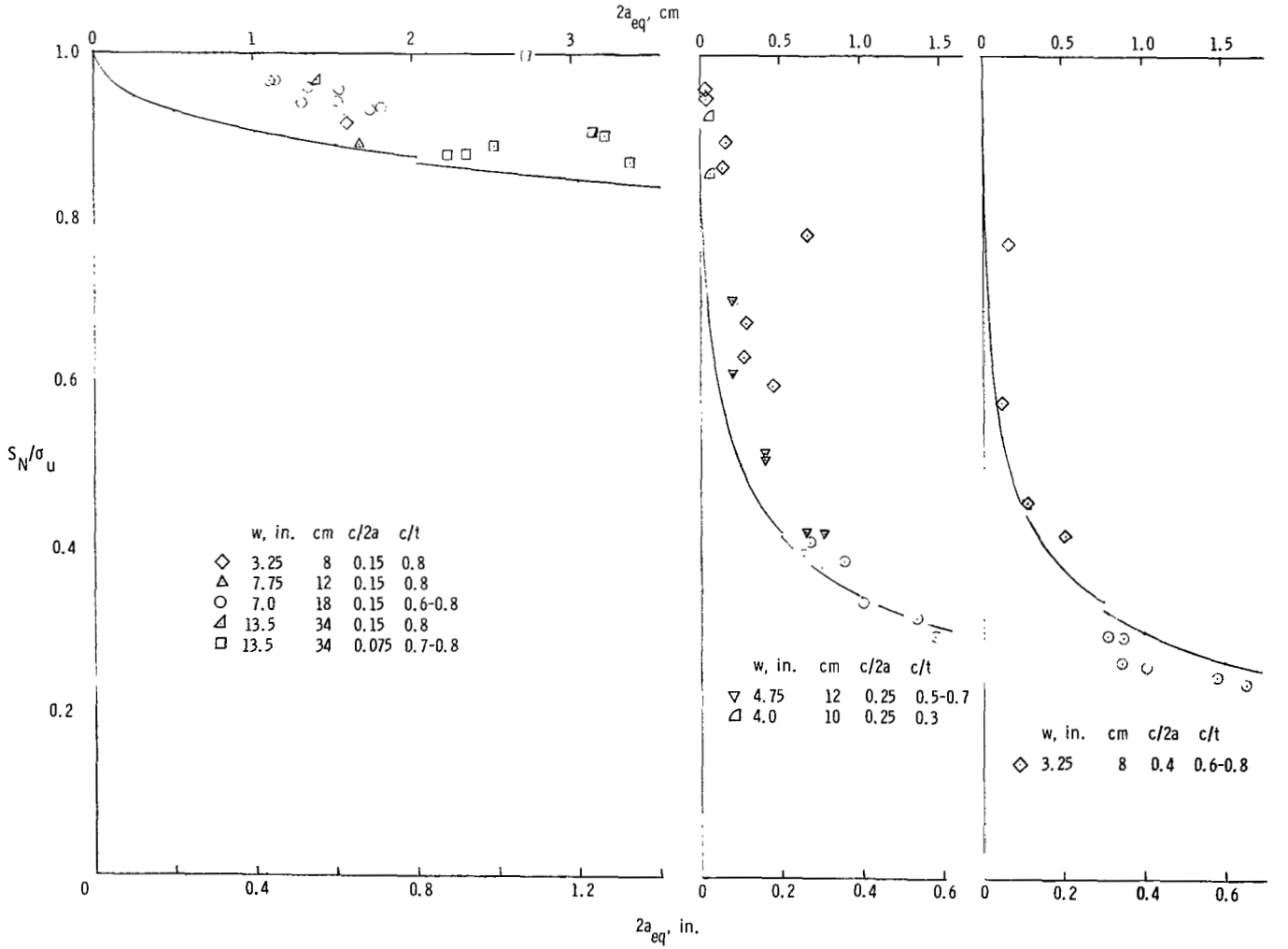

(a) Room temperature; σ_u = 115.7 ksi (796 MN/m^2); C_m = 0.257 in$^{-1/2}$ (0.161 cm$^{1/2}$) from one through-crack test with 2a = 15 in. (38 cm); w = 30 in. (76 cm).

(b) -320^0 F (77 K); σ_u = 185.5 ksi (1279 MN/m^2); C_m = 4.58 in$^{-1/2}$ (2.87 cm$^{-1/2}$) from one through-crack test with 2a = 4 in. (10 cm); w = 8 in. (20 cm).

(c) -423^0 F (20 K); σ_u = 205.7 ksi (1416 MN/m^2); C_m = 5.55 in$^{-1/2}$ (3.48 cm$^{-1/2}$) from one through-crack test with 2a = 4 in. (10 cm); w = 8 in. (20 cm).

Figure 7.- Surface-crack strength of Ti-5Al-2.5Sn alloy, transverse grain, t = 0.20 in. (5 mm). Test data taken from reference 5.

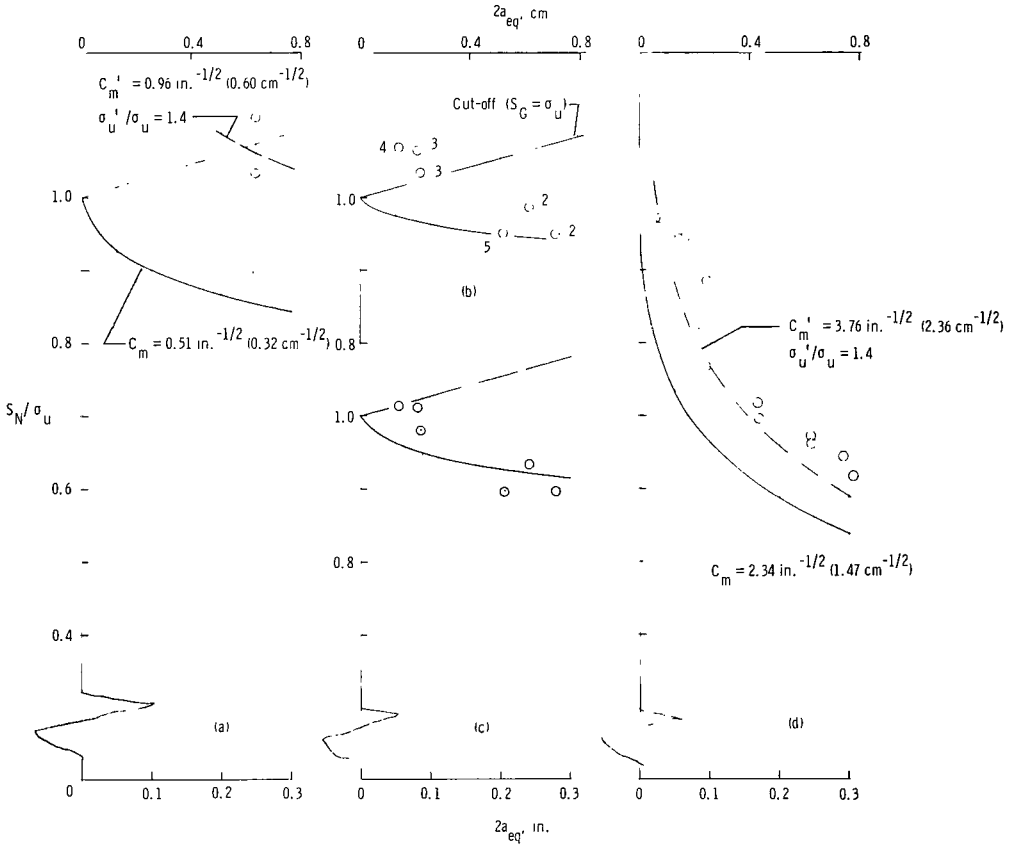

(a) Room temperature; σ_u = 116.6 ksi (803 MN/m^2); c/2a ≈ 0.05; c/t ≈ 0.9; C_m = 0.51 in$^{-1/2}$ (0.32 cm$^{-1/2}$) from one through-crack test with 2a = 15 in. (38 cm); w = 30 in. (76 cm).

(b) -320° F (77 K); σ_u = 179.6 ksi (1237 MN/m2) (coupon test value); c/2a ≈ 0.05 and 0.15; c/t ≈ 0.9; C_m = 0.176 in$^{-1/2}$ (0.110 cm$^{-1/2}$) from one through-crack test with 2a = 4 in. (10 cm) and w = 8 in. (20 cm).

(c) Test data as in figure 8(b), but σ_u assumed to be 1.053 times coupon test value. (See test for explanation.) C_m = 0.253 in$^{-1/2}$ (0.159 cm$^{-1/2}$).

(d) -423° F (20 K); σ_u = 205.6 ksi (1414 MN/m^2); c/2a ≈ 0.05 and 0.15; c/t ≈ 0.6 to 0.9. C_m and C_m' from one through-crack test with 2a = 4 in. (10 cm) and w = 8 in. (20 cm).

Figure 8.- Surface-crack strength of Ti-5Al-2.5Sn alloy, transverse grain, t = 0.02 in. (0.5 mm); w = 4 in. (10 cm); test data taken from reference 5.

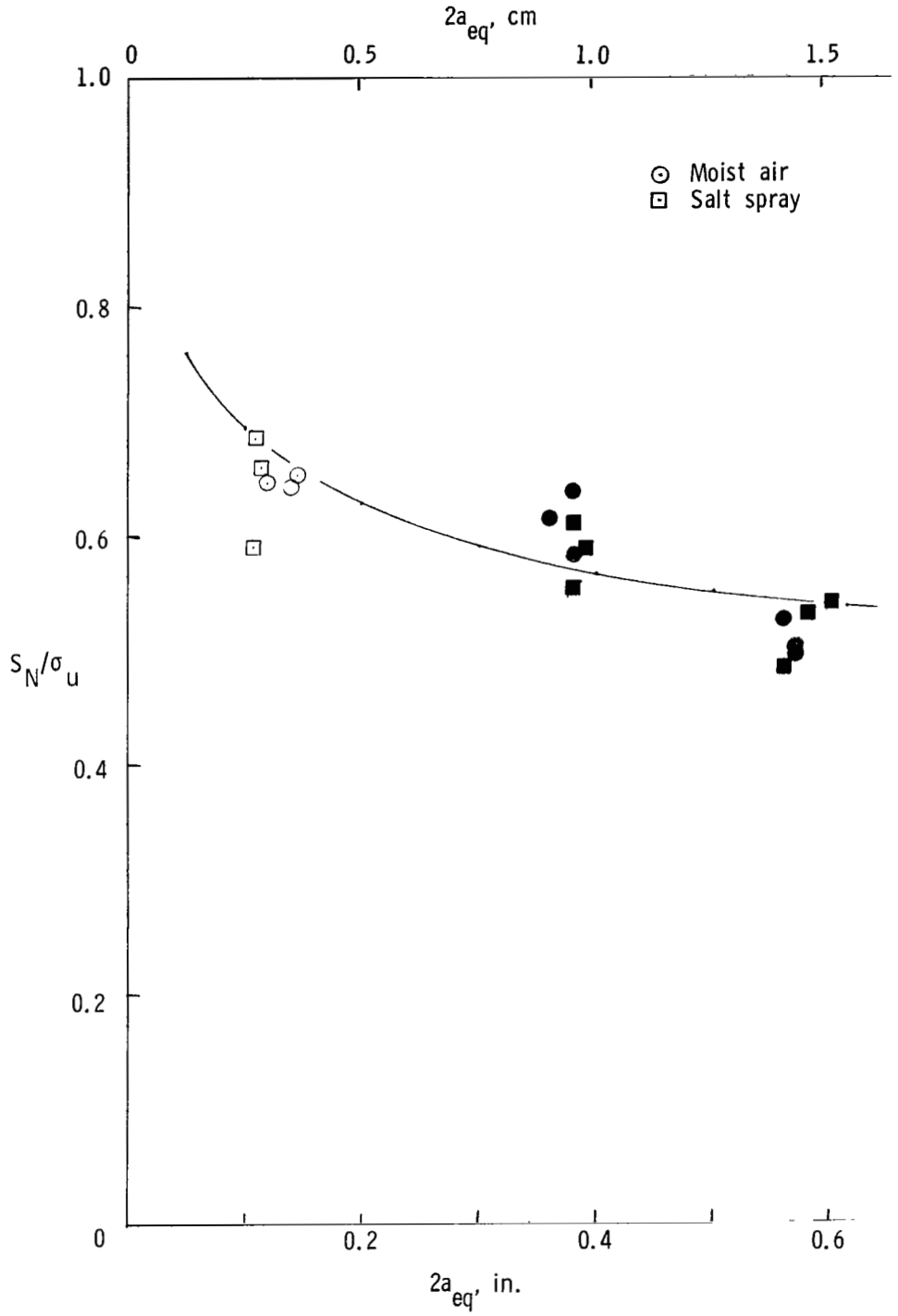

Figure 9.- Surface-crack strength of 300 M steel, longitudinal grain, t = 0.125 in. (3.2 mm). Room temperature; w = 2.25 in. (5.7 cm); $c/2a \approx 0.36$; $c/t \approx 0.8$; σ_u = 284.5 ksi (1961 MN/m^2); curve is calculated with $C_m = 2.05\ in^{-1/2}$ $(1.28\ cm^{-1/2})$, which is average result of three through-crack tests in moist air and three in salt spray with 2a = 1.2 to 2.6 in. (3 to 6.5 cm) and w = 5 in. (13 cm). Solid symbols denote surface-crack specimens which cracked through during fatigue cycling. Test data taken from reference 6.

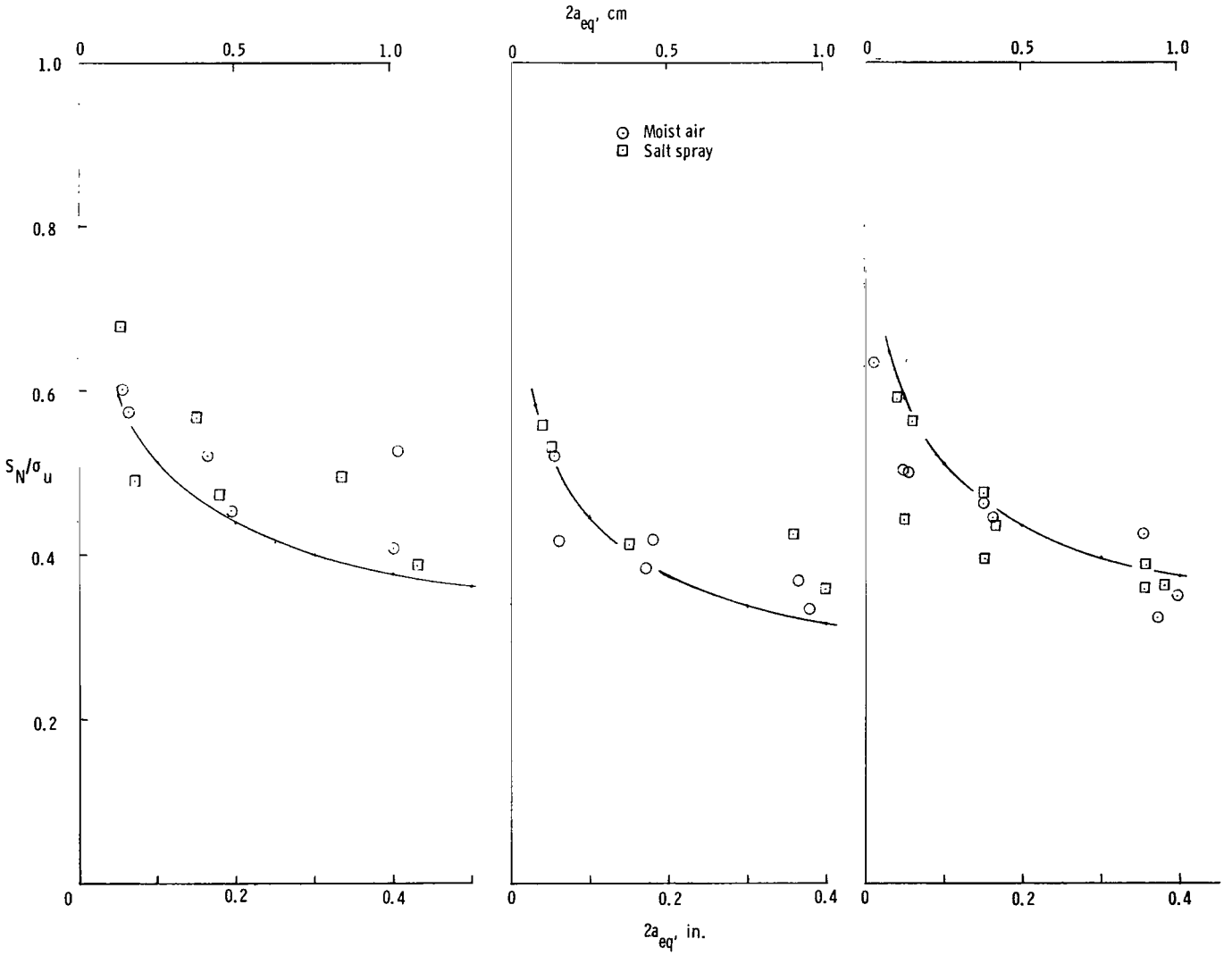

(a) σ_u = 229.5 ksi (1580 MN/m^2); C_m = 4.43 in$^{-1/2}$ (2.78 cm$^{-1/2}$).

(b) σ_u = 273 ksi (1880 MN/m^2); C_m = 5.86 in$^{-1/2}$ (3.65 cm$^{-1/2}$).

(c) σ_u = 286 ksi (1970 MN/m^2); C_m = 4.48 in$^{-1/2}$ (2.81 cm$^{-1/2}$).

Figure 10.- Surface-crack strength of 300 M steel, longitudinal grain, t = 0.375 in. (10 mm). Room temperature; w = 2.25 in. (5.7 cm); c/2a ≈ 0.4; c/t ≈ 0.8; C_m for each series determined from six through-crack tests in moist air and six tests in salt spray with 2a = 1.2 to 2.6 in. (3 to 6.5 cm) and w = 5 in. (13 cm).

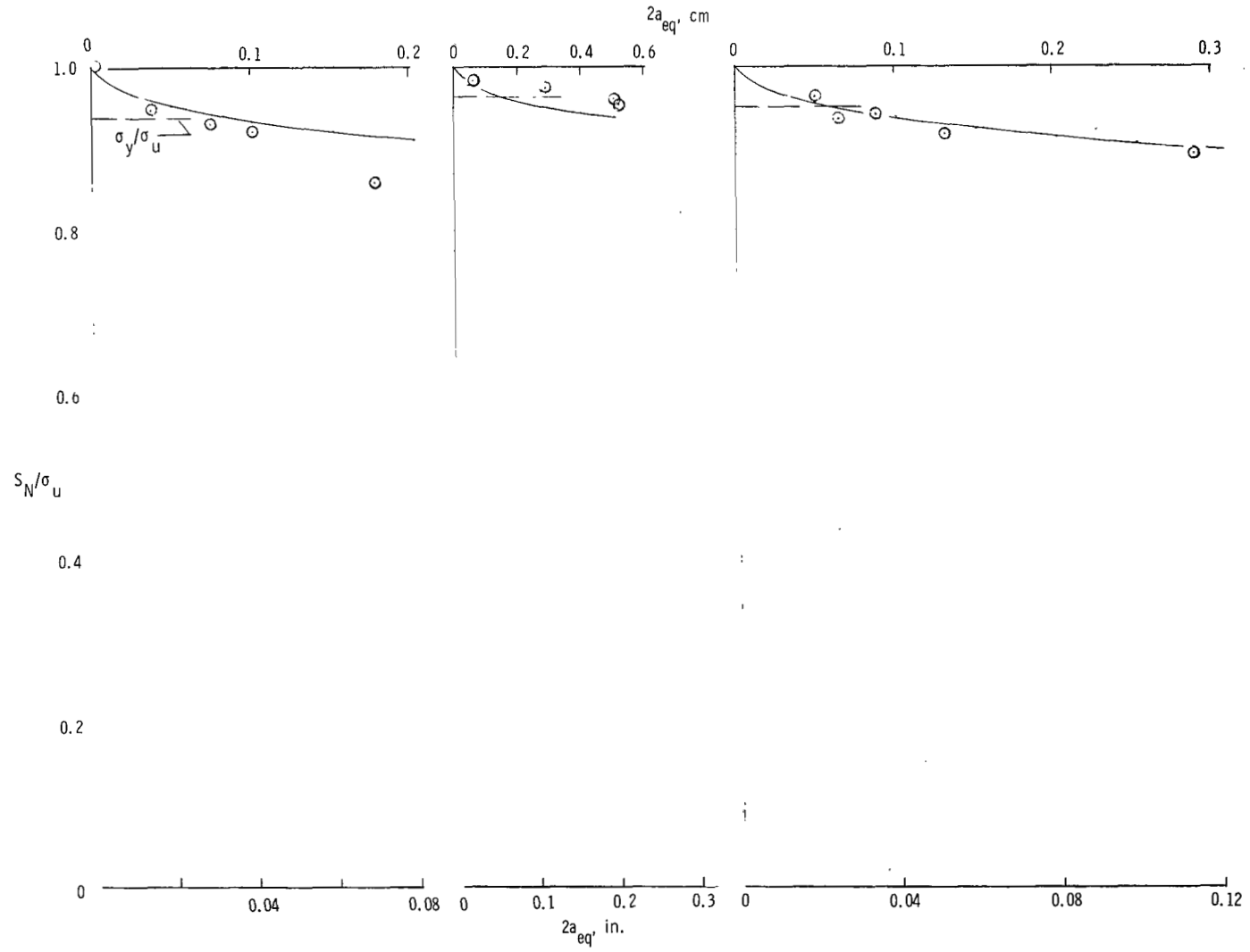

(a) Maraging 250 steel; t = 0.19 in. (5 mm); σ_u = 226.1 ksi (1559 MN/m^2); c/2a ≈ 0.3; c/t ≈ 0.06 to 0.5; C_m = 0.51 in$^{-1/2}$ (0.32 cm$^{-1/2}$).

(b) 9Ni-4Co steel; t = 0.19 in. (5 mm); σ_u = 206 ksi (1420 MN/m^2); c/2a ≈ 0.2 to 0.3; c/t ≈ 0.3 to 0.6; C_m = 0.23 in$^{-1/2}$ (0.14 cm$^{-1/2}$).

(c) Ti-6-6-2 annealed; t = 0.19 in. (5 mm); σ_u = 149.5 ksi (1030 MN/m^2); c/2a ≈ 0.2; c/t ≈ 0.3 to 0.5; C_m = 0.48 in$^{-1/2}$ (0.30 cm$^{-1/2}$).

Figure 11.- Correlation between through cracks and surface cracks for three materials. Room temperature tests; test data taken from reference 7. C_m determined for each material from two through-crack tests with w = 3 in. (7.6 cm) and 2a/w = 0.3. All surface-crack specimens; w = 3 in. (7.6 cm).

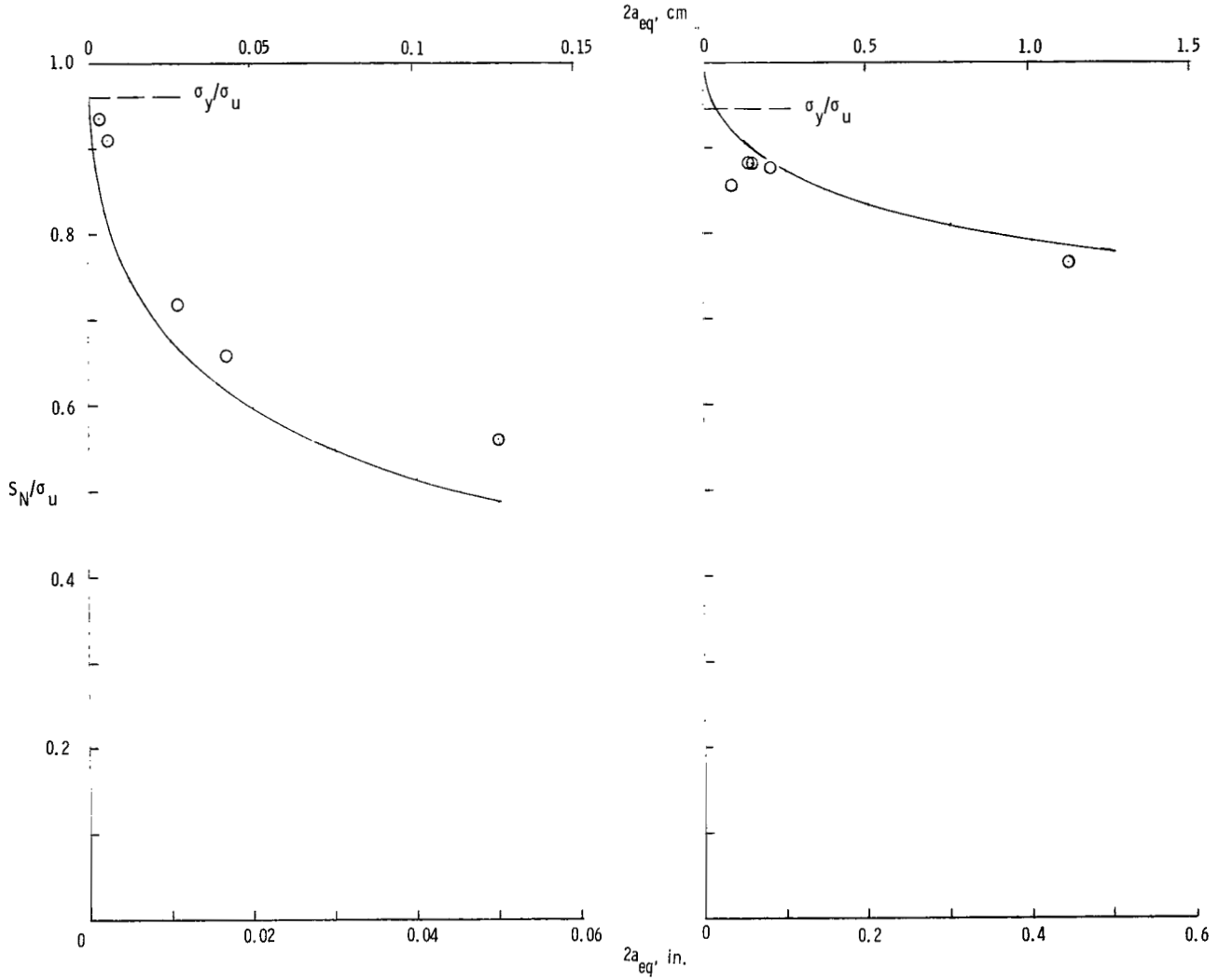

(a) PH-13-8Mo steel; t = 0.25 in. (6 mm); -110° F (194 K); σ_u = 228.4 ksi (1574 MN/m^2); c/2a ≈ 0.3; c/t ≈ 0.1 to 0.4; C_m = 6.80 in$^{-1/2}$ (4.26 cm$^{-1/2}$) from one through-crack test t = 0.183 in. (4.65 mm); w = 3 in. (7.6 cm); 2a/w ≈ 0.3 and one through-crack test t = 0.378 in. (9.60 mm); w = 6 in. (15.2 cm); 2a/w = 0.3.

(b) 4340 steel; t = 0.19 in. (5 mm); room temperature; σ_u = 225.6 ksi (1552 MN/m^2); c/2a ≈ 0.06 to 0.2; c/t ≈ 0.3 to 0.8; C_m = 0.68 in$^{-1/2}$ (0.43 cm$^{-1/2}$) from two through-crack tests with w = 3 in. (7.6 cm); 2a/w ≈ 0.3.

Figure 12.- Correlation between through cracks and surface cracks for two materials. Test data taken from reference 7. All surface-crack specimens w = 3 in. (7.6 cm).

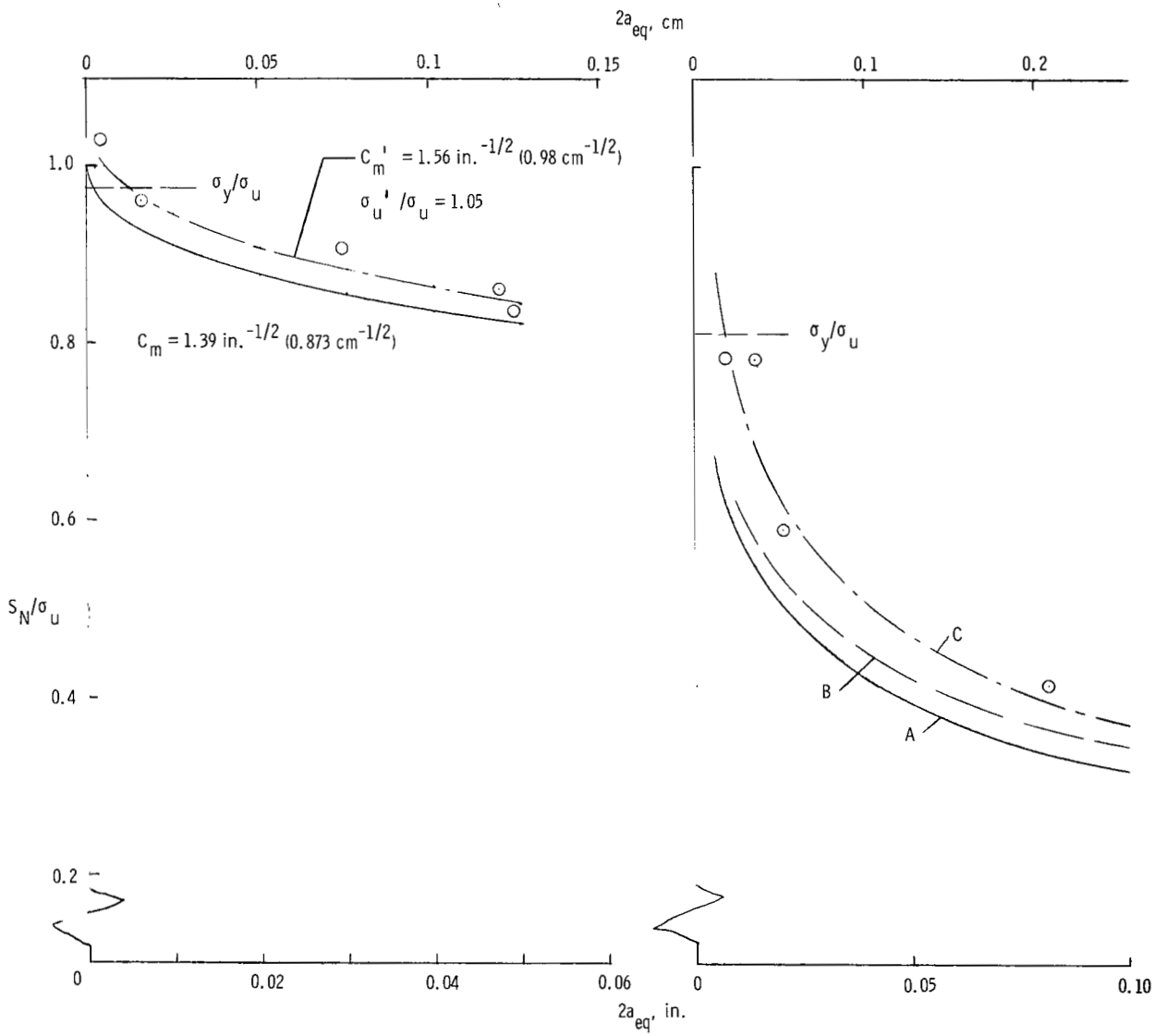

(a) Ti-6-4 alloy; t = 0.19 in. (5 mm); room temperature; σ_u = 160.1 ksi (1103 MN/m^2); w = 3 in. (7.6 cm); c/2a ≈ 0.25; c/t = 0.2 to 0.4. C_m and C_m' from two through-crack tests with w = 3 in. (7.6 cm) and 2a/w = 0.33.

(b) AM-355 steel; t = 0.19 in. (5 mm); -110^0 F (194 K); σ_u = 250 ksi (1722 MN/m^2); w = 3 in. (7.6 cm); c/2a ≈ 0.3; c/t = 0.2 to 0.6; for explanation of curves A, B, and C, see text.

Figure 13.- Correlation between through cracks and surface cracks for two materials. Test data taken from reference 7.

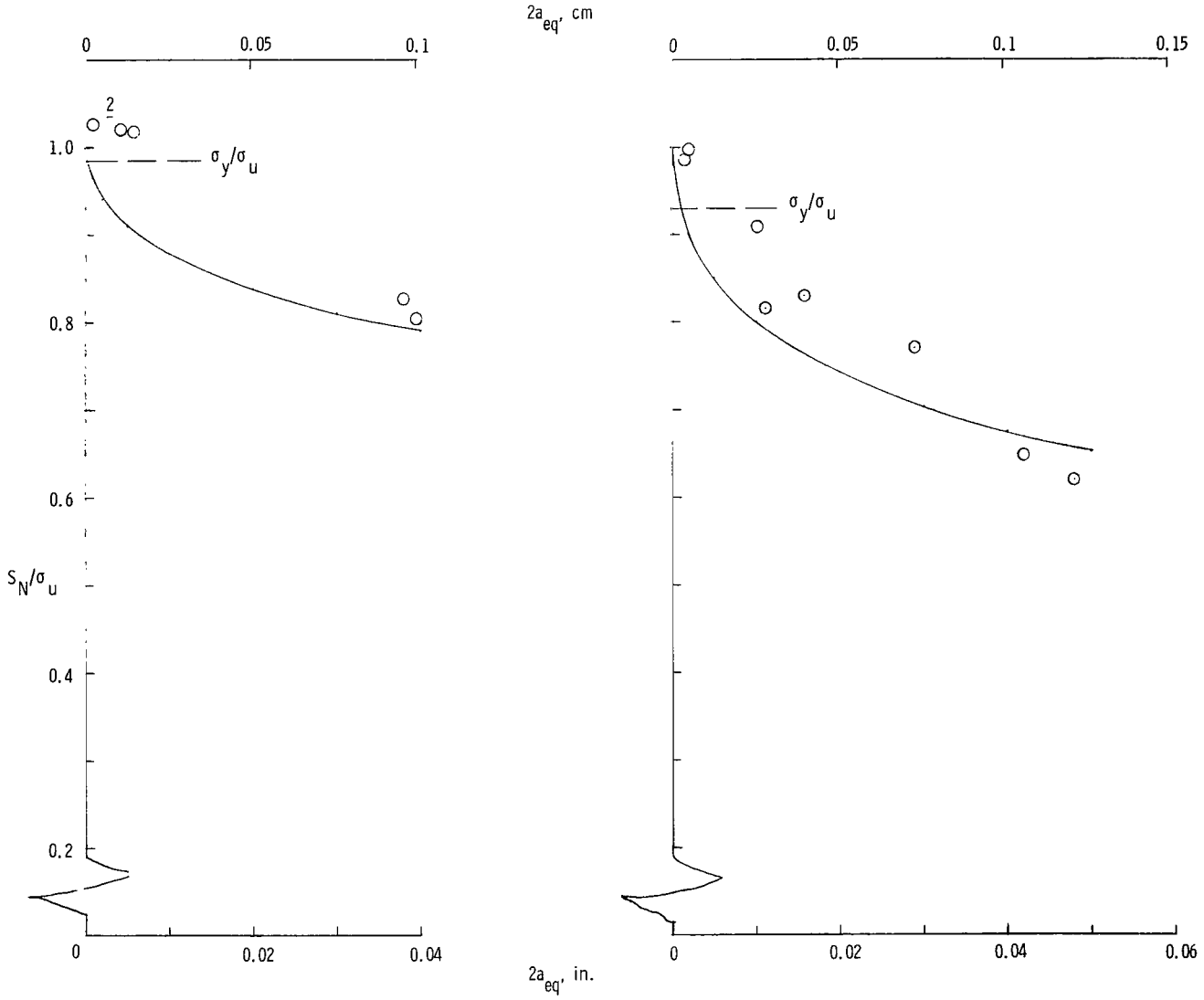

(a) 18 percent Ni steel; σ_u = 301 ksi (2075 MN/m^2); C_m = 1.97 in$^{-1/2}$ (1.235 cm$^{-1/2}$).

(b) Ti-6-4 alloy; σ_u = 180.5 ksi (1244 MN/m^2); C_m = 3.56 in$^{-1/2}$ (2.23 cm$^{-1/2}$).

Figure 14.- Correlation between through cracks and surface cracks for two materials. Test data taken from reference 8. t = 0.10 in. (2.5 cm); room temperature; w = 1 in. (2.54 cm); c/2a ≈ 0.3; c/t = 0.15 to 0.5. C_m for each material from three through-crack tests with 2a ≈ 0.5 in. (12 mm); w ≈ 1.6 in. (4 cm).

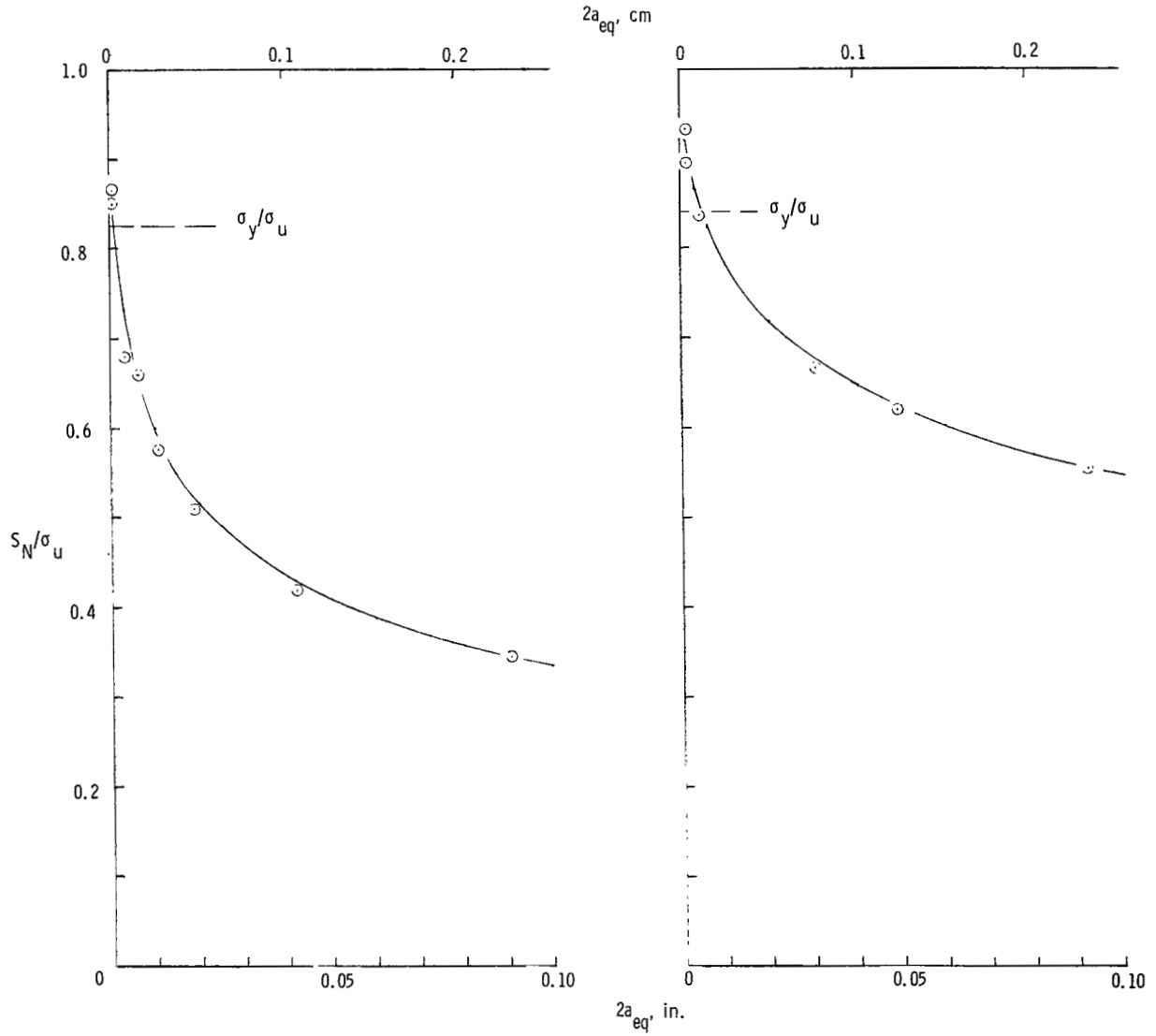

(a) 300 M (0.45 percent C) steel; σ_u = 291 ksi (2005 MN/m2); C_m = 9.50 $in^{-1/2}$ (5.95 $cm^{-1/2}$).

(b) 300 M (0.39 percent C) steel; σ_u = 287 ksi (1980 MN/m2); C_m = 3.96 $in^{-1/2}$ (2.48 $cm^{-1/2}$).

Figure 15.- Correlation of surface cracks for two materials. Test data taken from reference 6, appendix B. t = 0.20 in. (5 mm); room temperature; w = 1.5 in. (3.8 cm); c/2a = 0.2 to 0.5; c/t = 0.1 to 0.5.

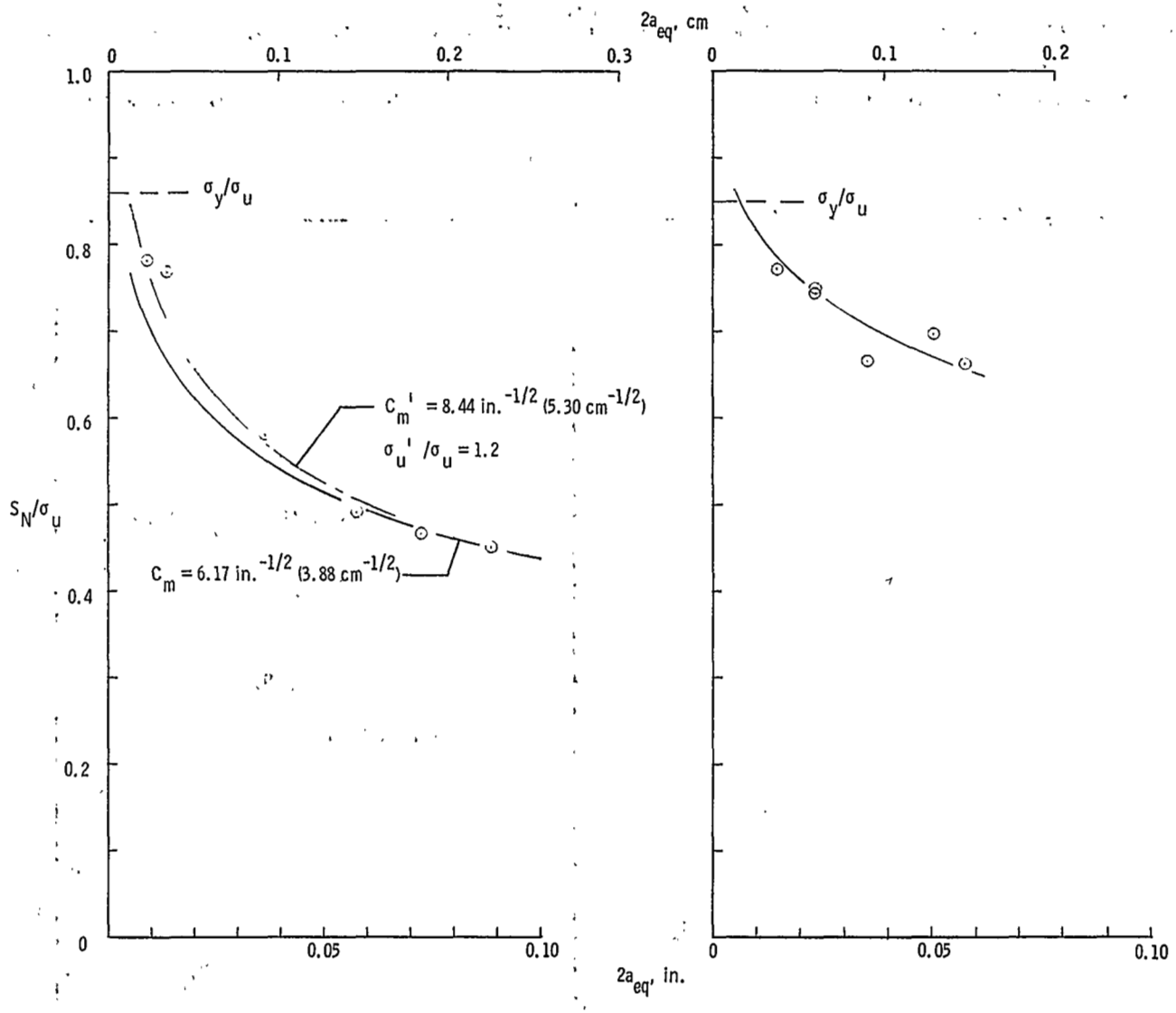

(a) 9NI-4CO martensitic steel; σ_u = 280 ksi (1930 MN/m^2).

(b) 9NI-4CO bainitic steel; σ_u = 275 ksi (1895 MN/m^2); C_m = 3.20 in$^{-1/2}$. (2.01 cm$^{-1/2}$).

Figure 16.- Correlation of surface cracks for two materials. Test data taken from reference 6, appendix B. t = 0.20 in. (5 mm); room temperature; w = 1.5 in. (3.8 cm); c/2a = 0.3 to 0.4; c/t = 0.3 to 0.5.

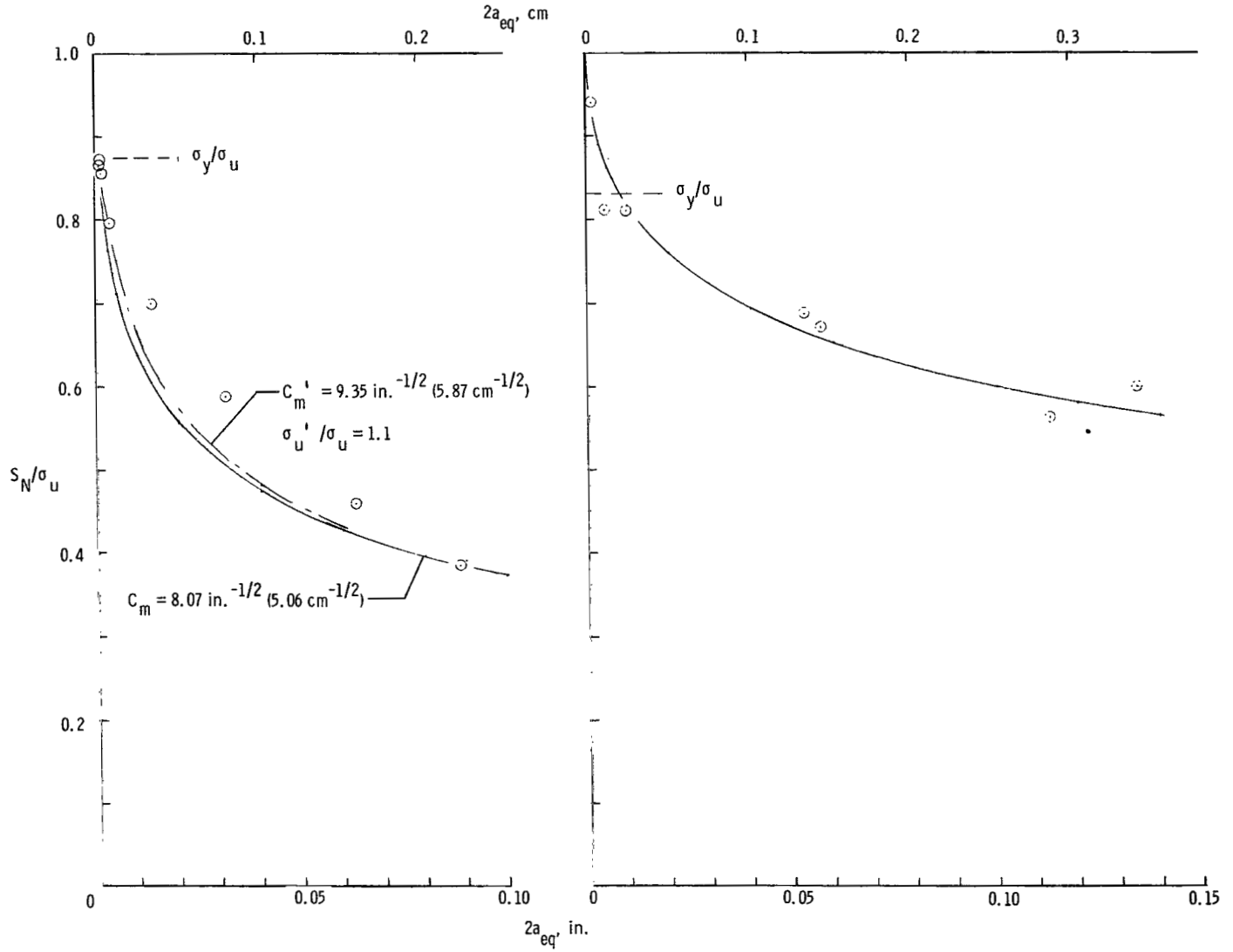

(a) D6 AC steel; σ_u = 279 ksi (1922 MN/m^2).

(b) 4340 steel; σ_u = 274 ksi (1890 MN/m^2); C_m = 3.20 in.$^{-1/2}$ (2.01 cm$^{-1/2}$).

Figure 17.- Correlation of surface cracks for two materials. Test data taken from reference 6, appendix B. t = 0.20 in. (5 mm); room temperature; w = 1.5 in. (3.8 cm); c/2a = 0.3 to 0.5; c/t = 0.1 to 0.6.

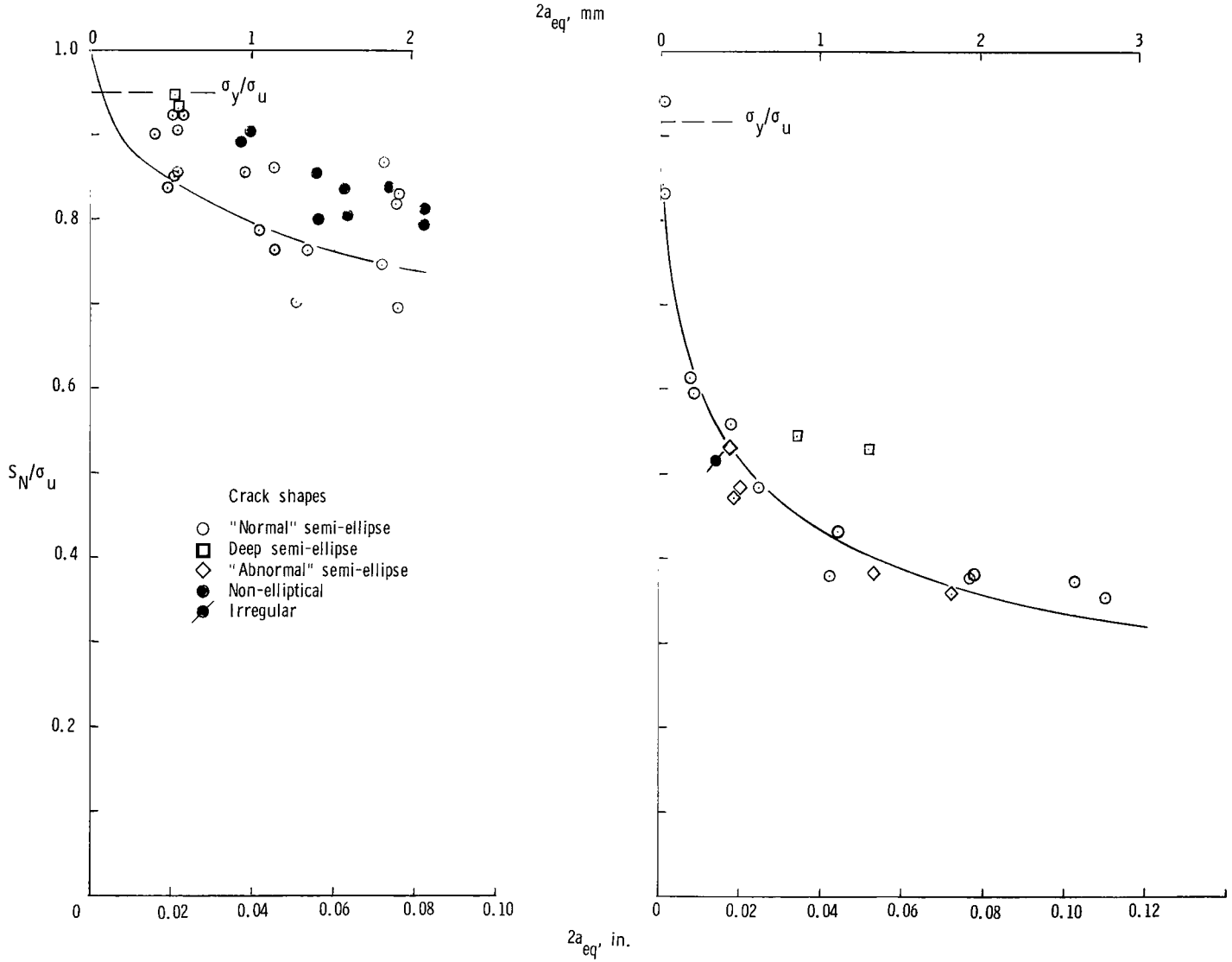

(a) σ_u = 162.5 ksi (1120 MN/m2); C_m = 1.86 $in^{-1/2}$ (1.17 $cm^{-1/2}$).

(b) σ_u = 174.5 ksi (1202 MN/m2); C_m = 9.50 $in^{-1/2}$ (5.95 $cm^{-1/2}$).

Figure 18.- Correlation of surface cracks for Ti 6-4 alloy in two heat-treat conditions. Test data taken from reference 9. t = 0.25 in. (6 mm); room temperature; w = 1.4 in. (3.6 cm).

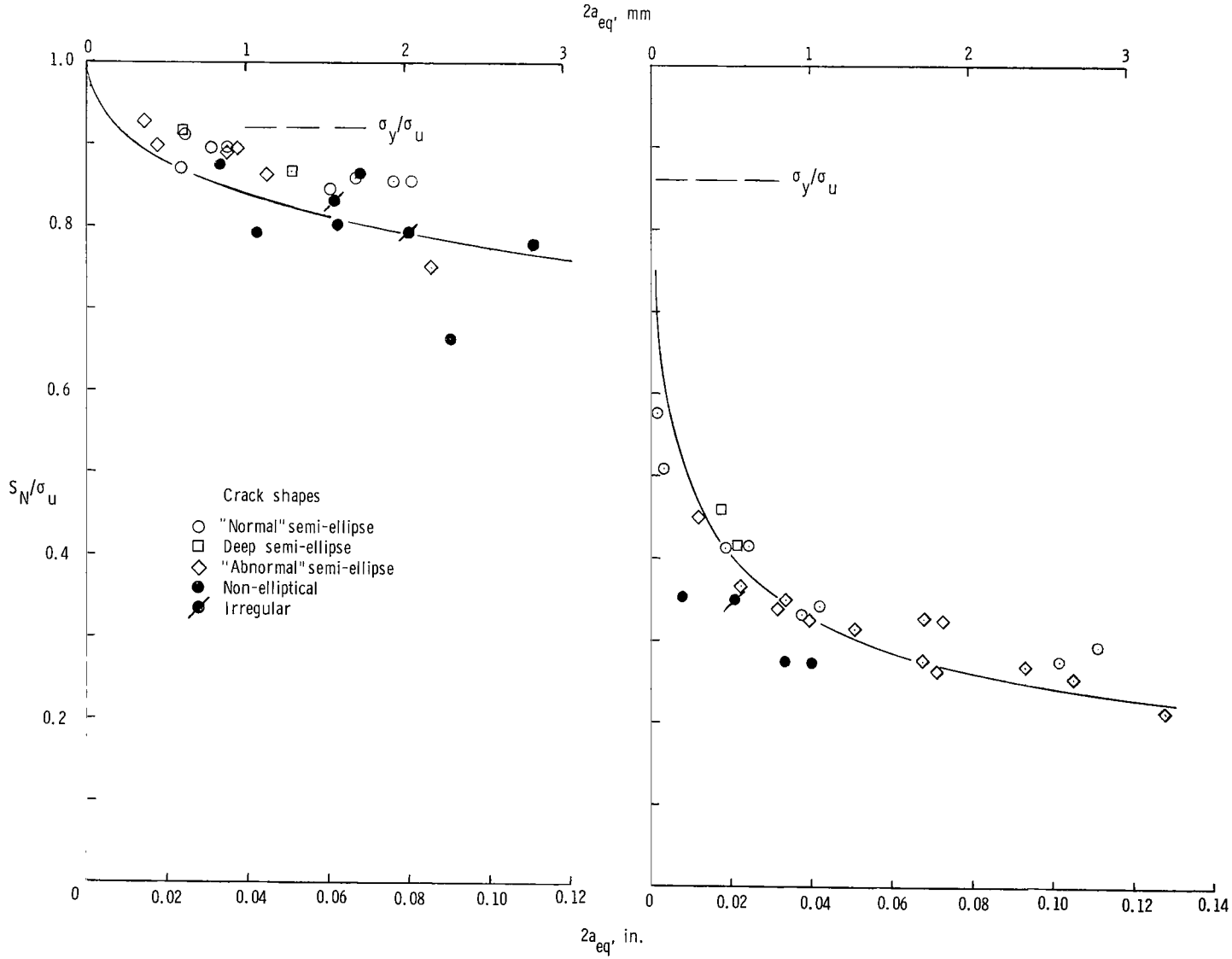

(a) σ_u = 229.5 ksi (1580 MN/m^2); C_m = 1.40 in$^{-1/2}$ (0.88 cm$^{-1/2}$).

(b) σ_u = 289 ksi (1990 MN/m^2); C_m = 15 in$^{-1/2}$ (9.4 cm$^{-1/2}$).

Figure 19.- Correlation of surface cracks for D6-AC steel in two heat-treat conditions. Test data taken from reference 9. t = 0.25 in. (6 mm); room temperature; w = 1.4 in. (3.6 cm).

"The aeronautical and space activities of the United States shall be conducted so as to contribute . . . to the expansion of human knowledge of phenomena in the atmosphere and space. The Administration shall provide for the widest practicable and appropriate dissemination of information concerning its activities and the results thereof."

— NATIONAL AERONAUTICS AND SPACE ACT OF 1958

NASA SCIENTIFIC AND TECHNICAL PUBLICATIONS

TECHNICAL REPORTS: Scientific and technical information considered important, complete, and a lasting contribution to existing knowledge.

TECHNICAL NOTES: Information less broad in scope but nevertheless of importance as a contribution to existing knowledge.

TECHNICAL MEMORANDUMS: Information receiving limited distribution because of preliminary data, security classification, or other reasons.

CONTRACTOR REPORTS: Scientific and technical information generated under a NASA contract or grant and considered an important contribution to existing knowledge.

TECHNICAL TRANSLATIONS: Information published in a foreign language considered to merit NASA distribution in English.

SPECIAL PUBLICATIONS: Information derived from or of value to NASA activities. Publications include conference proceedings, monographs, data compilations, handbooks, sourcebooks, and special bibliographies.

TECHNOLOGY UTILIZATION PUBLICATIONS: Information on technology used by NASA that may be of particular interest in commercial and other non-aerospace applications. Publications include Tech Briefs, Technology Utilization Reports and Notes, and Technology Surveys.

Details on the availability of these publications may be obtained from:

SCIENTIFIC AND TECHNICAL INFORMATION DIVISION

NATIONAL AERONAUTICS AND SPACE ADMINISTRATION

Washington, D.C. 20546